tee to Revise the 1995 Guidelines for the Evaluation and Management of Heart Failure): Developed in Collaboration With the International Society for Heart and Lung Transplantation; Endorsed by the Heart Failure Society of America. *Circulation* 104: 2996–3007, 2001.

10. **Ide T, Tsutsui H, Kinugawa S, Suematsu N, Hayashidani S, Ichikawa K, Utsumi H, Machida Y, Egashira K, and Takeshita A.** Direct evidence for increased hydroxyl radicals originating from superoxide in the failing myocardium. *Circ Res* 86: 152–157, 2000.
11. **Ishibashi N, Weisbrot-Lefkowitz M, Reuhl K, Inouye M, and Mirochnitchenko O.** Modulation of chemokine expression during ischemia/reperfusion in transgenic mice overproducing human glutathione peroxidases. *J Immunol* 163: 5666–5677, 1999.
12. **Jesmin S, Sakuma I, Hattori Y, Fujii S, and Kitabatake A.** Long-acting calcium channel blocker benidipine suppresses expression of angiogenic growth factors and prevents cardiac remodelling in a Type II diabetic rat model. *Diabetologia* 45: 402–415, 2002.
13. **Jessup M and Brozena S.** Heart failure. *N Engl J Med* 348: 2007–2018, 2003.
14. **Kakkar R, Kalra J, Mantha SV, and Prasad K.** Lipid peroxidation and activity of antioxidant enzymes in diabetic rats. *Mol Cell Biochem* 151: 113–119, 1995.
15. **Kanazawa A, Nishio Y, Kashiwagi A, Inagaki H, Kikkawa R, and Horiike K.** Reduced activity of mtTFA decreases the transcription in mitochondria isolated from diabetic rat heart. *Am J Physiol Endocrinol Metab* 282: E778–E785, 2002.
16. **Kinugawa S, Tsutsui H, Hayashidani S, Ide T, Suematsu N, Satoh S, Utsumi H, and Takeshita A.** Treatment with dimethylthiourea prevents left ventricular remodeling and failure after experimental myocardial infarction in mice: role of oxidative stress. *Circ Res* 87: 392–398, 2000.
17. **Knollmann BC, Blatt SA, Horton K, de Freitas F, Miller T, Bell M, Housmans PR, Weissman NJ, Morad M, and Potter JD.** Inotropic stimulation induces cardiac dysfunction in transgenic mice expressing a troponin T (I79N) mutation linked to familial hypertrophic cardiomyopathy. *J Biol Chem* 276: 10039–10048, 2001.
18. **Le CT, Hollaar L, van der Valk EJ, and van der Laarse A.** Buthionine sulfoximine reduces the protective capacity of myocytes to withstand peroxide-derived free radical attack. *J Mol Cell Cardiol* 25: 519–528, 1993.
19. **Litwin SE, Raya TE, Anderson PG, Daugherty S, and Goldman S.** Abnormal cardiac function in the streptozotocin-diabetic rat. Changes in active and passive properties of the left ventricle. *J Clin Invest* 86: 481–488, 1990.
20. **Mirochnitchenko O, Palnitkar U, Philbert M, and Inouye M.** Thermosensitive phenotype of transgenic mice overproducing human glutathione peroxidases. *Proc Natl Acad Sci USA* 92: 8120–8124, 1995.
21. **Mizushige K, Yao L, Noma T, Kiyomoto H, Yu Y, Hosomi N, Ohmori K, and Matsuo H.** Alteration in left ventricular diastolic filling and accumulation of myocardial collagen at insulin-resistant prediabetic stage of a type II diabetic rat model. *Circulation* 101: 899–907, 2000.
22. **Nakatani T, Inouye M, and Mirochnitchenko O.** Overexpression of antioxidant enzymes in transgenic mice decreases cellular ploidy during liver regeneration. *Exp Cell Res* 236: 137–146, 1997.
23. **Nishikawa T, Edelstein D, Du XL, Yamagishi S, Matsumura T, Kaneda Y, Yorek MA, Beebe D, Oates PJ, Hammes HP, Giardino I, and Brownlee M.** Normalizing mitochondrial superoxide production blocks three pathways of hyperglycaemic damage. *Nature* 404: 787–790, 2000.
24. **Norton GR, Candy G, and Woodiwiss AJ.** Aminoguanidine prevents the decreased myocardial compliance produced by streptozotocin-induced diabetes mellitus in rats. *Circulation* 93: 1905–1912, 1996.
25. **Riva E, Andreoni G, Bianchi R, Latini R, Luvara G, Jeremic G, Traquandi C, and Tuccinardi L.** Changes in diastolic function and collagen content in normotensive and hypertensive rats with long-term streptozotocin-induced diabetes. *Pharmacol Res* 37: 233–240, 1998.
26. **Rosen P, Ballhausen T, Bloch W, and Addicks K.** Endothelial relaxation is disturbed by oxidative stress in the diabetic rat heart: influence of tocopherol as antioxidant. *Diabetologia* 38: 1157–1168, 1995.
27. **Shiomi T, Tsutsui H, Ikeuchi M, Matsusaka H, Hayashidani S, Suematsu N, Wen J, Kubota T, and Takeshita A.** Streptozotocin-induced hyperglycemia exacerbates left ventricular remodeling and failure after experimental myocardial infarction. *J Am Coll Cardiol* 42: 165–172, 2003.
28. **Shiomi T, Tsutsui H, Matsusaka H, Murakami K, Hayashidani S, Ikeuchi M, Wen J, Kubota T, Utsumi H, and Takeshita A.** Overexpression of glutathione peroxidase prevents left ventricular remodeling and failure after myocardial infarction in mice. *Circulation* 109: 544–549, 2004.
29. **Siwik DA, Pagano PJ, and Colucci WS.** Oxidative stress regulates collagen synthesis and matrix metalloproteinase activity in cardiac fibroblasts. *Am J Physiol Cell Physiol* 280: C53–C60, 2001.
30. **Siwik DA, Tzortzis JD, Pimental DR, Chang DL, Pagano PJ, Singh K, Sawyer DB, and Colucci WS.** Inhibition of copper-zinc superoxide dismutase induces cell growth, hypertrophic phenotype, and apoptosis in neonatal rat cardiac myocytes in vitro. *Circ Res* 85: 147–153, 1999.
31. **Toussaint O, Houbion A, and Remacle J.** Relationship between the critical level of oxidative stresses and the glutathione peroxidase activity. *Toxicology* 81: 89–101, 1993.
32. **Twigg SM, Cao Z, McLennan SV, Burns WC, Brammar G, Forbes JM, and Cooper ME.** Renal connective tissue growth factor induction in experimental diabetes is prevented by aminoguanidine. *Endocrinology* 143: 4907–4915, 2002.
33. **Vasan RS, Benjamin EJ, and Levy D.** Prevalence, clinical features and prognosis of diastolic heart failure: an epidemiologic perspective. *J Am Coll Cardiol* 26: 1565–1574, 1995.
34. **Welt K, Fitzl G, and Schepper A.** Experimental hypoxia of STZ-diabetic rat myocardium and protective effects of Ginkgo biloba extract. II. Ultrastructural investigation of microvascular endothelium. *Exp Toxicol Pathol* 52: 503–512, 2001.
35. **Yamamoto K, Masuyama T, Sakata Y, Nishikawa N, Mano T, Yoshida J, Miwa T, Sugawara M, Yamaguchi Y, Ookawara T, Suzuki K, and Hori M.** Myocardial stiffness is determined by ventricular fibrosis, but not by compensatory or excessive hypertrophy in hypertensive heart. *Cardiovasc Res* 55: 76–82, 2002.
36. **Ye G, Metreveli NS, Ren J, and Epstein PN.** Metallothionein prevents diabetes-induced deficits in cardiomyocytes by inhibiting reactive oxygen species production. *Diabetes* 52: 777–783, 2003.
37. **Young ME, McNulty P, and Taegtmeyer H.** Adaptation and maladaptation of the heart in diabetes: Part II: potential mechanisms. *Circulation* 105: 1861–1870, 2002.

Thyroid Hormone Inhibits Vascular Remodeling Through Suppression of cAMP Response Element Binding Protein Activity

Kae Fukuyama, Toshihiro Ichiki, Ikuyo Imayama, Hideki Ohtsubo, Hiroki Ono, Yasuko Hashiguchi, Akira Takeshita, Kenji Sunagawa

Objective—Although accumulating evidences suggest that impaired thyroid function is a risk for ischemic heart disease, the molecular mechanism of anti-atherosclerotic effects of thyroid hormone is poorly defined. We examined whether thyroid hormone affects signaling pathway of angiotensin II (Ang II), which is critically involved in a broad aspect of cardiovascular disease process.

Methods and Results—3,3′,5-triiodo-L-thyronine (T3) did not show a significant effect on Ang II-induced activation of extracellular signal-regulated protein kinase or p38 mitogen-activated protein kinase in vascular smooth muscle cells (VSMCs), whereas T3 inhibited Ang II-induced activation of cAMP response element (CRE) binding protein (CREB), a nuclear transcription factor involved in the vascular remodeling process. Coimmunoprecipitaion assay revealed the protein-protein interaction between thyroid hormone receptor and CREB. T3 reduced an expression level of interleukin (IL)-6 mRNA, CRE-dependent promoter activity, and protein synthesis induced by Ang II. Administration of T3 (100 μg/100 g for 14 days) to rats attenuated neointimal formation after balloon injury of carotid artery with reduced CREB activation and BrdU incorporation.

Conclusion—These results suggested that T3 inhibits CREB/CRE signaling pathway and suppresses cytokine expression and VSMCs proliferation, which may account for, at least in part, an anti-atherosclerotic effect of thyroid hormone. (*Arterioscler Thromb Vasc Biol.* **2006;26:2049-2055.**)

Key Words: angiotensin II ■ cAMP response element binding protein ■ thyroid hormone ■ vascular remodeling

Thyroid hormone has various effects on the cardiovascular system. Hypothyroidism is known to be associated with accelerated atherosclerosis and coronary artery disease.[1,2] The Rotterdam study showed that subclinical hypothyroidism is a risk factor for atherosclerosis and myocardial infarction independently of total cholesterol level.[3] It was shown that more angiographic progression of coronary atherosclerosis was documented in patients with the lower serum thyroid hormone level after 2 years of observation.[2,4] These results suggest that thyroid hormone is protective against atherosclerosis; however, the molecular mechanism of anti-atherosclerotic effects has remained to be elucidated.

3,3′,5-triiodo-L-thyronine (T3) is an active form of thyroid hormone, which binds to thyroid hormone receptor (TR). The activated TR recruits transcriptional co-activators and induces gene expression through binding to thyroid hormone response element (TRE) in the promoter region of thyroid hormone responsive genes.[5]

Angiotensin II (Ang II) has multiple biological functions and is involved in a broad aspect of cardiovascular disease process. There are 2 isoforms for Ang II receptor designated type 1 receptor (AT_1R) and type 2 receptor (AT_2R). AT_1R mediates most of the traditional biological effects of Ang II, including vasoconstriction, water and sodium retention, and hypertrophy and hyperplasia of vascular smooth muscle cells (VSMCs). We previously reported that Ang II induced IL-6 expression and vascular hypertrophy through cAMP response element-binding protein (CREB).[6,7] CREB is a 43-kDa nuclear transcription factor bound to cAMP response element (CRE).[8,9] The functional state of CREB is regulated by phosphorylation of serine residue at 133 (Ser133), which promotes association with transcriptional co-activator proteins, CREB-binding protein (CBP) and p300. Overexpression of dominant negative CREB, of which serine 133 is replaced with alanine, attenuated neointimal formation after balloon injury of rat carotid artery.[10]

A recent study showed a physical interaction between TR and CREB[11] in fibroblasts. However, it is not clear whether this novel signaling cross talk affects the vascular remodeling process. We examined the effect of T3 on Ang II signaling pathway and the vascular remodeling process.

Original received December 30, 2005; final version accepted June 5, 2006.

From the Department of Cardiovascular Medicine, Kyushu University Graduate School of Medical Sciences, Fukuoka, Japan.

Consulting Editor for this article was Alan M. Fogelman, MD, Professor of Medicine and Executive Chair, Department of Medicine and Cardiology, UCLA School of Medicine, Los Angeles, Calif.

Correspondence to Toshihiro Ichiki, Department of Cardiovascular Medicine, Kyushu University Graduate School of Medical Sciences, 3-1-1 Maidashi, Higashi-ku, 812-8582 Fukuoka, Japan. E-mail ichiki@cardiol.med.kyushu-u.ac.jp

Arterioscler Thromb Vasc Biol. **is available at http://www.atvbaha.org** **DOI: 10.1161/01.ATV.0000233358.87583.01**

Materials and Methods

Materials

Dulbecco's modified Eagle's medium (DMEM) and fetal bovine serum was purchased from GIBCO BRL. Bovine serum albumin, T3 and an anti-α tubulin antibody were purchased from Sigma-Aldrich, Inc. Ang II was purchased from Peninsula Laboratories, Inc. [^{3}H]-leucine and [^{32}P]α-dCTP were purchased from PerkinElmer Life Sciences. Horseradish peroxidase-conjugated secondary antibodies (anti-rabbit and anti-mouse IgG) were purchased from VECTOR Laboratories Inc. An anti thyroid hormone receptor (anti-TR) antibody that recognizes both TRα and TRβwere purchased from Santa Cruz Biotechnology, Inc. Other antibodies used in the experiments were obtained from Cell Signaling Technology. Other chemical reagents were purchased from Wako Pure chemicals unless specifically mentioned.

Cell Culture

VSMCs were isolated from the thoracic aorta of Sprague-Dawley rats (Kyudo Co; Kamamoto, Japan). Passages between 5 and 13 were used for the experiments as described previously.[6]

Animals

All procedures and care were approved by the Committee on Ethics of Animal Experiments, Kyushu University, and were conducted according to animal care guidelines of the American Physiological Society. Adult male, 12 to 13-week-old Sprague-Dawley rats (350 to 400 g) were anesthetized by intraperitoneal injection of pentobarbital sodium. The left common carotid artery was denuded of the endothelium with a 2-Fr Fogarty balloon catheter (Baxter) that was introduced through the external carotid artery. Inflation and retraction of the balloon catheter were repeated 3 times. Then rats received intraperitoneal injection of T3 (100 μg/100 g body weight suspended in 0.02 N NaOH) every other day for 2 weeks (Hyperthyroid group). Control group received injection of 0.02 N NaOH. Systolic blood pressure and heart rate were measured using tail-cuff method (UR-5000, UEDA). After 2 weeks, rats were euthanized under pentobarbital anesthesia. Carotid arteries were quickly removed and blood samples were collected. Serum concentrations of T3, T4 and thyroid-stimulating hormone (TSH) were measured by radioimmunoassay.

Common carotid artery was ligated just proximal of the bifurcation. The extent of neointimal formation in the just proximal portion of the ligation was examined histologically.

Morphometry and Immunohistochemistry

Serial cross-sections of the carotid rings were stained with hematoxylin and eosin and subjected to morphometry for assessing the intima-media area ratio (I/M ratio) and to immunohistochemistry with the use of the denoted primary antibody and a commercially available detection system as described previously.[10]

Detection of Apoptosis and DNA Synthesis In Vivo

Apoptotic cells were detected by the terminal deoxynucleotidyl transferase (TdT)-mediated dUTP nick end-labeling (TUNEL) method with an apoptosis in situ detection kit (Wako Pure Chemicals) as described previously.[10] In vivo labeling with BrdU (0.5 mg/kg), a thymidine analogue that was injected intraperitoneally 3 hours before preparation of the artery, was performed to identify replicating cells by detection of DNA synthesis. The incorporated BrdU was detected immunohistochemically with an anti-BrdU antibody (Cell proliferation kit, Amersham Pharmacia Biotech) as described previously.[10]

Western Blot Analysis

VSMCs were lysed and Western blot analyses of CREB, extracellular signal-regulated protein kinase (extracellular signal regulated kinase [ERK]) and p38 mitogen-activated protein kinase (p38-MAPK) were performed as described previously.[7]

Immunoprecipitations

VSMCs were lysed in NP-40 lysis buffer[12] and immunoprecipitated with a primary antibody (specific for TR or CREB). Immunoprecipitated proteins were electrophoresed on 12% SDS-PAGE as described previously.[12] An antibody against CREB or TR was used for immunoblotting.

Northern Blot Analysis

Total RNA was prepared according to an acid guanidinium-thiocyanate-phenol-chloroform extraction method. Northern blot analysis for IL-6 and 18S rRNA were performed as described previously.[13]

Measurement of CRE-Dependent Promoter Activity

VSMCs (5×10^5) were prepared in a 6-cm tissue culture dish; 5 μg of CRE (3 copies) /luciferase fusion DNA construct with thymidine kinase (TK) promoter and 2 μg of LacZ gene (driven by simian virus 40 promoter-enhancer sequence) were introduced to VSMCs with the DEAE-dextran method according to the manufacturer's instruction (Promega Corporation). VSMCs were cultured in DMEM with 10% fetal bovine serum for 24 hours, and then incubated with T3 for 30 minutes and stimulated with Ang II (1μmol/L) for 24 hours in DMEM containing 0.1% bovine serum albumin. The luciferase activity was measured and normalized by β-galactosidase activity as described previously.[13]

Measurement of Protein Synthesis

VSMCs were preincubated with T3 for 30 minutes and stimulated with Ang II for 1 hour. Then the medium was changed to a fresh DMEM with 0.1% bovine serum albumin and incubated for additional 23 hours. The cells were labeled with [^{3}H]-leucine during the last 12 hours. Incorporation of [^{3}H]-leucine was measured by a liquid scintillation counter as described previously.[14]

Statistical Analysis

Statistical analysis was performed with 1-way ANOVA and Fisher test if appropriate. Data are shown as mean±SEM. $P<0.05$ was considered to be statistically significant.

Results

T3 Suppressed Ang II-Induced Phosphorylation of CREB at Ser133

We previously reported that Ang II induced CREB activation with a peak at 5 minutes.[7] VSMCs were preincubated with T3 for 30 minutes and stimulated with Ang II for 5 minutes. Western blot analysis using an antibody against phosphorylated form of CREB at Ser133 (P-CREB) was performed. T3 suppressed Ang II-induced phosphorylation of CREB in a dose-dependent manner (Figure 1A). Expression level of total CREB (lower panel) was not affected either by Ang II or T3.

T3 Suppressed CRE-Dependent Transcription Induced by Ang II

A luciferase reporter construct driven by 3 copies of CRE and TK promoter (Figure 1B, left) was introduced VSMCs and luciferase activity was examined. Ang II increased CRE-dependent promoter activity after 24 hours of stimulation, and T3 suppressed the effect of Ang II (Figure 1B).

T3 Had Minimal Effect on Ang II-Induced MAPKs Activation

Ang II induced CREB activation is dependent on ERK and p38MAPK.[7] T3 slightly inhibited the Ang II-induced ERK or

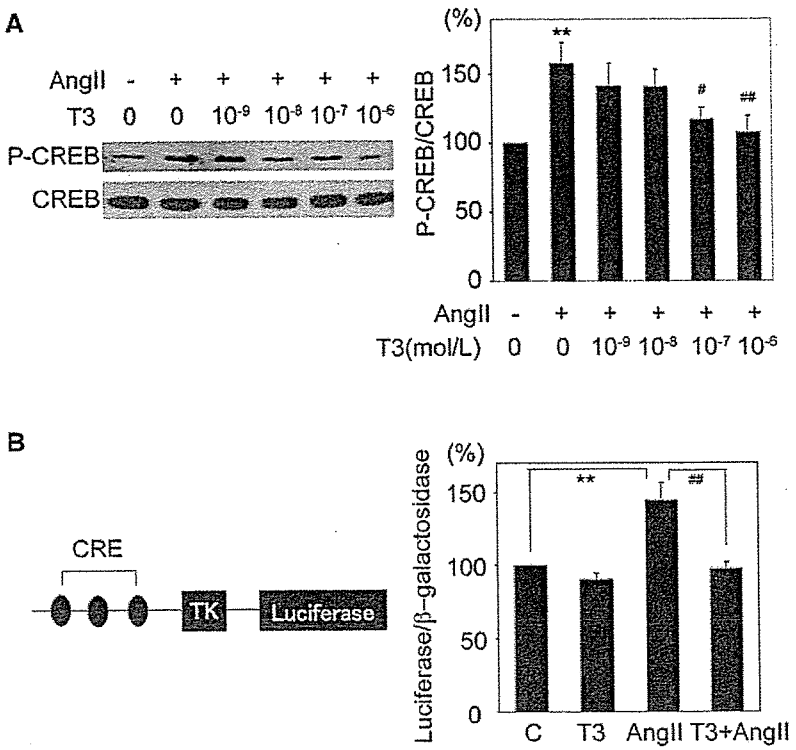

Figure 1. T3 suppressed Ang II-induced phosphorylation of CREB at Ser133. A, VSMCs were preincubated with T3 for 30 minutes at concentrations varying from 10^{-9} to 10^{-6} mol/L and stimulated with Ang II (10^{-7} mol/L) for 5 minutes (n=10). Phosphorylation of CREB was detected by Western blot analysis using a phospho-specific CREB antibody. Density of the specific band was scanned and quantified with an imaging analyzer. The ratio of phosphorylated CREB to total CREB is shown in the right panel. The values (mean±SEM) are expressed as a percent of control (100%). $^{**}P<0.01$ vs control, $^{\#\#}P<0.01$ vs Ang II-stimulated cell, $\#P<0.5$ vs Ang II-stimulated cell. B, CRE (3 copies) /luciferase fusion DNA construct with thymidine kinase promoter (TK) is shown in left panel. The construct and LacZ gene were introduced to VSMCs with the DEAE-dextran method. VSMCs were preincubated with T3 (10^{-6} mol/L) for 30 minutes and stimulated with Ang II (10^{-6} mol/L) for 24 hours (n=4). The luciferase activity was normalized by the β-galactosidase activity. Relative luciferase activity of unstimulated VSMCs (control) was set as 100%. Mean±SEM, $^{**}P<0.01$, $^{*}P<0.05$, $\#\#P<0.01$ vs Ang II-stimulated cell.

p38MAPK phosphorylation as shown in figure 2A and 2B. However, densitometric analysis revealed that inhibition of MAPK phosphorylation by T3 is statistically insignificant (Ang II versus T3+Ang II, pERK; $P=0.182$, p38MAPK; $P=0.135$). Therefore, it was suggested that MAPK does not play a pivotal role in the T3-induced inhibition of CREB phosphorylation.

CREB Interacts With Thyroid Hormone Receptor

Recently, it has been suggested that T3 induced a direct protein–protein interaction between TR and CREB.[11] Immunoprecipitation analysis revealed that CREB was coimmunoprecipitated with TR and vice versa (Figure 2C). However, the amount of associated protein was almost the same between T3-stimulated cells (T3) and nonstimulated cells (C), suggesting that CREB and TR are constitutively interacting.

T3 Suppressed Angiotensin II-Induced IL-6 Expression

It was examined whether T3-induced inhibition of CREB results in the suppression of Ang II-induced gene expression. Preincubation with T3 for 30 minutes reduced the expression level of Ang II-induced IL-6 mRNA, which is dependent on CRE and CREB[6] (Figure 3A).

T3 Inhibited Angiotensin II-Induced Protein Synthesis in VSMCs

The effect of T3 on Ang II-induced incorporation of [^{3}H]-leucine was examined. We previously reported that prolonged expose (>3 hours) to T3 reduced AT_1R expression level in VSMCs.[15] To exclude the possible effect of T3 inhibition of AT_1R expression on Ang II-induced leucine incorporation, the medium was changed to a fresh serum free medium after VSMCs were preincubated with T3 for 30 minutes and stimulated with Ang II for additional 1 hour. Ang II weakly but significantly increased protein synthesis with 1 hour of stimulation and T3 inhibited Ang II-induced protein synthesis (Figure 3B).

Neointimal Formation of Balloon-Injured Artery Was Suppressed in Hyperthyroid Rats

We previously showed that inhibition of CREB function attenuated neointimal formation after vascular injury.[10] We assumed that T3 might show the same effect if T3 inhibits CREB function in vivo. We treated rats with T3 after balloon injury (Table). After 14 days of balloon injury of rat carotid artery, the cross-section of carotid artery showed a substantial neointimal formation (Figure 4A, left). Administration of T3 significantly suppressed the neointimal formation (Figure 4A,

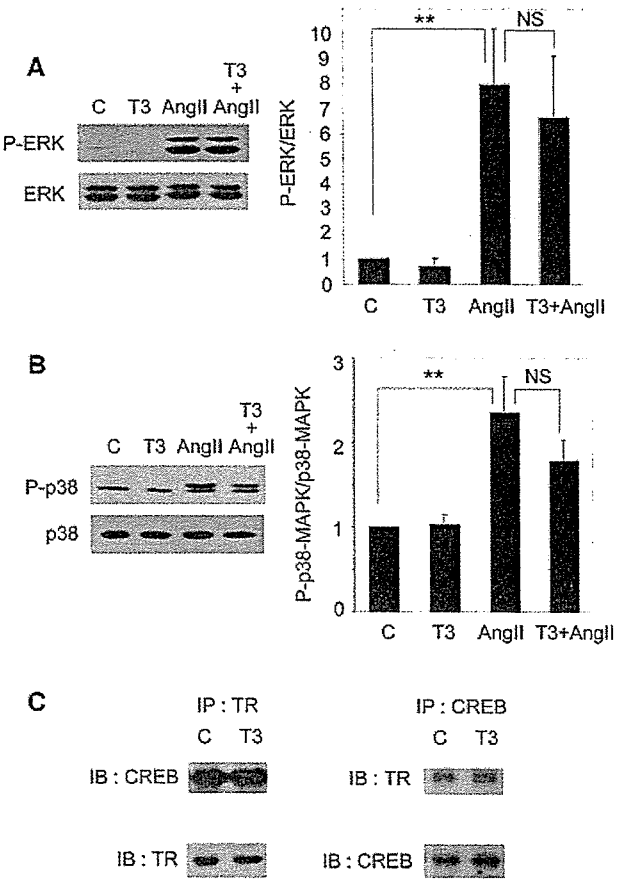

Figure 2. An effect of T3 on Ang II-induced MAP kinase activation. VSMCs were preincubated with T3 (10^{-6} mol/L) for 30 minutes and stimulated with Ang II (10^{-7} mol/L) for 5 minutes. Western blot analysis of (A) phosphorylated ERK (P-ERK) and ERK (n=6), (B) phosphorylated p38-MAPK (P-p38), and p38-MAPK (n=7) were performed as described in the legend to Figure 1. Density of the specific band was scanned and quantified with an imaging analyzer. The ratio of phosphorylated ERK to total ERK and phosphorylated p38-MAPK to total p38-MAPK are shown. $^{**}P<0.05$, NS=not significant. C, VSMCs were stimulated with T3 (10^{-6} mol/L) for 30 minutes, lysed and immunoprecipitated (IP) with an antibody specific to TR (left panel) or an antibody specific to CREB (right panel). Both TR and CREB were detected by immunoblot analysis (IB) as described in the legend to Figure 1. A representative autoradiograph is shown. (n=6)

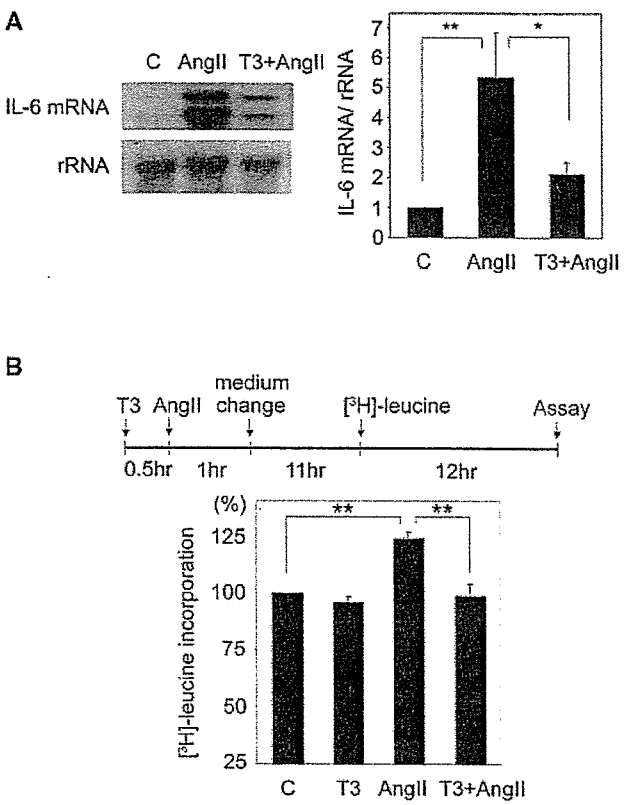

Figure 3. Effects of T3 on Ang II-induced IL-6 mRNA expression and protein synthesis. A, VSMCs were preincubated with T3 (10^{-6} mol/L) for 30 minutes and stimulated with Ang II (10^{-6} mol/L) for another 30 minutes. IL-6 mRNA expression was detected by Northern blot analysis. The radioactivity of the band of IL-6 mRNA was counted by a Bioimage Analyzer and was normalized by that of rRNA. The ratio of radioactivity of IL-6 mRNA to that of rRNA is shown (n=6). The values are expressed as mean±SEM. $^{**}P<0.01$, $^{*}P<0.05$. B, VSMCs were preincubated with T3 (10^{-6} mol/L) for 30 minutes and stimulated with Ang II (10^{-7} mol/L) for 1 hour. The medium was changed to fresh serum free medium and incubated for additional 23 hours. The protocol is shown in the upper panel. Incorporation of [^{3}H]-leucine was measured by a liquid scintillation counter. Results are expressed as mean±SEM. [^{3}H]-leucine incorporation of unstimulated cells was set as 100%. n=9, $^{**}P<0.01$.

right and, 4B). CREB-positive and phosphorylated CREB-positive cells were detected in the neointima of the carotid arteries (Figure 4C). T3 reduced the ratio of phosphorylated CREB positive cells to total cells (Figure 4C upper right panel), whereas the ratio of CREB positive cells to total cells was not changed (Figure 4C lower right panel).

To examine whether T3 induces apoptosis in neointima of balloon-injured artery or not, we detected apoptotic cells with TUNEL method. Although TUNEL index (the ratio of TUNEL positive cells to total cells) were slightly increased in T3-treated rats compared with control, the increase was not statistically significant (Figure 5A). BrdU positive cells were increased in the neointima after 7 days of vascular injury. In T3-treated rats, BrdU labeling index was lower than control group (5.27±1.46% versus 9.73±1.89% in control, $P<0.05$), which suggests that T3 decreased cell proliferation in the neointima of balloon-injured artery (Figure 5B). To exclude the possible effect of high blood flow on the neointimal formation in hyperthyroid state, we examined the extent of neointimal formation in a carotid artery ligation model. The I/M ratio of hyperthyroid rats was also decreased compared with that of control rats in this model (Figure I, available online at http://atvb.ahajournals.org), suggesting that thyroid hormone inhibits neointimal formation, at least in part, through a direct effect on the blood vessel.

Discussion

Ang II plays an important role in atherosclerotic cardiovascular disease and is known to accelerate atherogenesis through vascular hypertrophy, cytokine production, and cell growth.[16–18] Many reports have shown that MAPKs are critically involved in these processes.[7,19] We previously

Physiological Characteristics and Serum Hormone Concentration

	Control		T3-Treated	
	0 Days	14 Days	0 Days	14 Days
Body weight, g	320±11.9	365±5.3*	332±9.9	297±7.6*‡
Blood pressure, mm Hg	130±3.5	127±3.4	123±4.2	134±2.9
Heart rate, beat/min	367±12.7	378±13.7	363±8.9	522±10.4†‡
TSH, ng/mL		7.68±0.48		5.45±0.16§
Free T3, pg/mL		0.78±0.02		6.85±5.79
Free T4, ng/dL		3.34±0.24		1.67±0.08§

TSH indicates thyroid stimulating hormone; T3, triiodothyronine; T4, thyroxine.

n=6. *P<0.05, †P<0.01 vs 0 day, ‡P<0.01 vs control, §P<0.01 vs control.

demonstrated that Ang II induced CREB activation through ERK and p38-MAPK pathways.[7] In this study, we reported an inhibitory effect of T3 on Ang II-induced CREB phosphorylation (Figure 1). T3, however, showed insignificant effects on ERK or p38-MAPK activation. Although we could not exclude the possibility that the T3-induced mild attenuation of MAPK phosphorylation affect CREB phosphorylation, the coimmunoprecipitation assay suggests that protein-protein interaction between CREB and TR may play a role (Figure 3). To our knowledge, this is the first report to show an existence of crosstalk between Ang II signaling and T3 signaling in VSMC.

Contradicting results are reported in terms of the effect of thyroid hormone on intracellular cAMP level. Marchal et al[20] reported that T3 increased cAMP production in myoblasts. In contrast, it was reported that T3 or T4 inhibited basal and corticotropin (ACTH)-stimulated levels of intracellular cAMP in adrenal cells.[21] Incubation with T3 alone did not affect the phosphorylation level of CREB (data not shown) or CRE-dependent gene transcription (Figure 1B) in our VSMCs. These data may suggest that cAMP level is not affected by T3 in VSMCs and the effect of thyroid hormone on cAMP level may be cell type-dependent.

Ang II is involved in vascular remodeling after balloon injury. It is reported that AT_1R mediates the progression of neointimal thickening after balloon-injured artery in rat.[22,23] We showed that hyperthyroidism downregulated AT_1R in the aorta in the previous study.[15] It was also demonstrated that T3 suppressed CREB phosphorylation and decreased cell proliferation in the neointima of balloon-injured artery. Therefore the decreased AT_1R level may be responsible for the decreased CREB phosphorylation and neointimal formation. However, in vitro study clearly demonstrated that T3 inhibited CREB phosphorylation with 30 minutes' of preincubation, which is insufficient to downregulate AT_1R. It may be, therefore, plausible to assume that both downregulation of AT_1R and inhibition of CREB phosphorylation are responsible for the reduced neointimal formation in T3-treated rats. However, it is difficult to examine these two effects separately in vivo.

We previously reported that overexpression of dominant negative CREB in injured rat carotid artery attenuated neointimal formation[10] with increased apoptosis and decreased

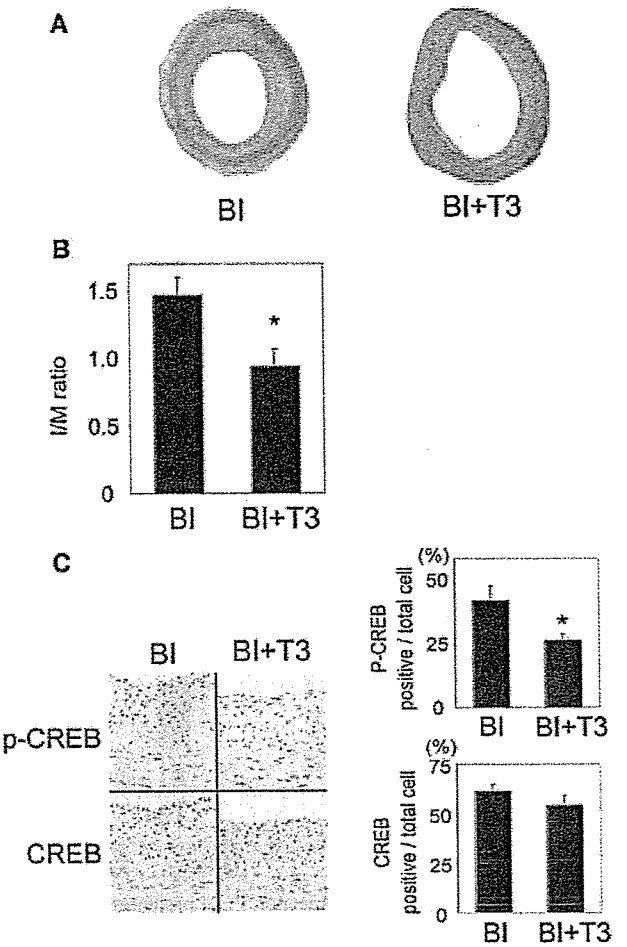

Figure 4. Neointimal formation of balloon-injured artery was suppressed in hyperthyroid rats. A, Representative microphotographs of hematoxylin-eosin staining of carotid arteries after 14 days of balloon injury (BI) are shown. In the right panel, rats received intraperitoneal injection of T3 (100 μg/100 g body weight suspended in 0.02 N NaOH) every other day for 2 weeks after BI (BI+T3). In the left panel, BI group received injection of 0.02 N NaOH only. B, A bar graph shows I/M ratio in the BI and BI+T3 groups. C, Representative microphotographs of immunohistochemistry for CREB and phosphorylated CREB in injured carotid artery at 14 days after injury are shown at left panel. The ratio of phosphorylated CREB-positive or CREB-positive cell number to total cell number is shown in the right panel (n=7).

proliferation. Although we expected that T3 has the same effect on injured artery, a significant increase in TUNEL index was not observed. This is probably because thyroid hormone has other effects than inhibiting CREB activity on blood vessel. And incubation of VSMCs with T3 for 24 hours failed to inhibit Ang II-induced CREB phosphorylation (data not shown). Further study is needed to clarify the mechanisms of these differences.

There are several reports describing that nuclear receptors can modulate gene expression by mechanism of protein–protein interaction with other transcription factors. Tagami et al reported an involvement of CREB in negative regulation of TSHα promoter activity by T3.[24] They suggests that T3 induces release of the co-repressor/histone deacetylase (HDAC) complex from TR and recruits co-activators such as

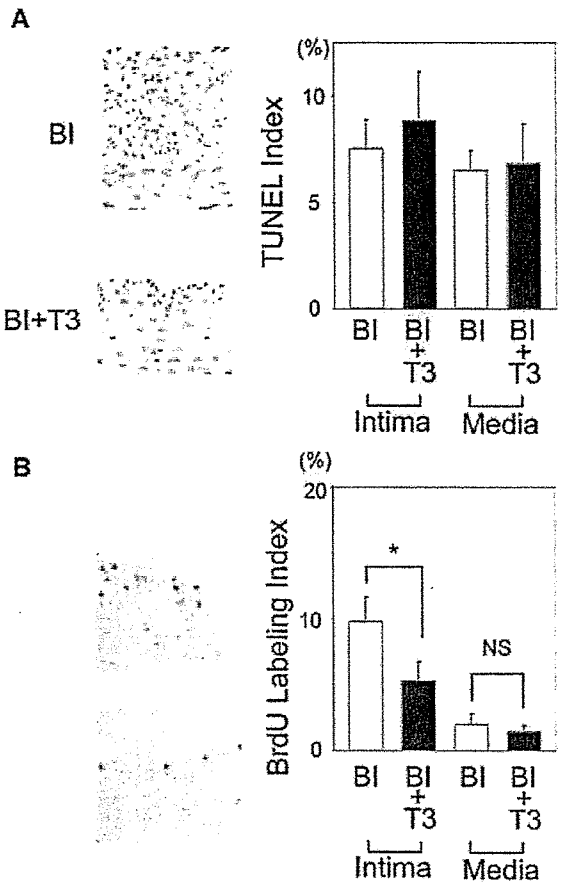

Figure 5. Effect of T3 on apoptosis and cell proliferation after balloon injury. A, TUNEL was performed in the cross-section of carotid arteries after 14 days of balloon injury with (BI+T3) or without (BI) T3 treatment (n=7). Representative microphotographs are shown in left panel and TUNEL index of intima or media is indicated in right panel. B, Representative microphotographs of BrdU labeling in the cross sections of carotid arteries after 7 days of balloon injury with (BI+T3) or without (BI) T3 treatment are shown in left panel. BrdU labeling index of intima or media is indicated in right panel. Results are expressed as mean±SEM (n=6). *$P<0.05$. NS=not significant.

CBP to TR, which competes CBP away from the CREB on the promoter, causing repression of CREB-dependent transcription. It is also reported that the co-repressor complex containing HDAC released from TR binds to other transcription factors such as Octamer transcription factor-1 (Oct-1)[25] and nuclear factor-κB (NF-κB),[26] and inhibits the Oct-1–dependent or NF-κB–dependent gene transcription. Tricostatin A (TSA), an inhibitor of HDAC, is reported to restore co-repressor-induced suppression of IL-2 gene expression that is activated by NF-κB. We examined whether TSA abolishes T3-dependent suppression of Ang II-induced IL-6 expression. However, TSA did not affect T3 inhibition of Ang II-induced IL-6 mRNA expression (data not shown), suggesting that corepressor complex may not be involved. Recently, Mendez-Pertuz et al reported a transcriptional cross-talk between CREB and TR signaling pathways.[11] They showed that overexpression of CREB reduced T3-dependent transcriptional activation. To clarify the role of CREB, we took an advantage of overexpression of wild-type CREB by an adenovirus vector. Overexpression of CREB, however, did not restore an inhibitory effect of T3 on Ang II-induced IL-6 mRNA expression and Ang II-induced protein synthesis (data not shown). This may suggest that CREB is abundantly expressed in VSMCs. Actually, CREB is a ubiquitously expressed transcription factor and one report suggested that all the CRE sites in the genome are saturated by endogenous CREB.[27]

In this report, we showed a ligand-independent interaction between CREB and TR. T3 did not change the amount of association of CREB with TR but inhibited Ang II-induced CREB phosphorylation, which suggests that T3 may cause conformational change of TR resulting in the inhibition of CREB phosphorylation.

In the present study, we used a relatively high concentration of T3 to stimulate VSMCs. However, Mizuma et al[28] have shown the presence of an iodothyronine deiodinase in human VSMCs. This suggests that VSMCs are able to convert T4 to T3 and that intracellular concentration of T3 in blood vessel may be higher than the serum concentration. In addition, plasma concentration of T3 was not so high and TSH was weakly suppressed in our hyperthyroid model (Table), indicating that neointimal formation was significantly reduced in the mild hyperthyroid state. We therefore believe that our results are clinically relevant.

In summary, T3 inhibited Ang II-induced CREB activation without affecting MAPK activation. T3 attenuated Ang II-induced cytokine expression and protein synthesis. Neointimal formation of balloon-injured artery was suppressed in T3-treated rats with reduced CREB activation and cell proliferation. These results may suggest that an antiatherosclerotic effect of thyroid hormone is, at least in part, dependent on the inhibition of AT_1R signaling and expression.

Sources of Funding

This study was supported in part by grants from Kimura Memorial Research Foundation, Takeda Science Foundation and a Grant-in-aid for Scientific Research from ministry of Education, Culture, Sports, Science, and Technology of Japan. (17590742).

Disclosures

None.

References

1. Vanhaelst L, Neve P, Bastenie PA. Coronary-artery disease in myxoedema. *Lancet.* 1967;2:1257–1258.
2. Barth JD, Jansen H, Kromhout D, Reiber JH, Birkenhager JC, Arntzenius AC. Progression and regression of human coronary atherosclerosis. The role of lipoproteins, lipases and thyroid hormones in coronary lesion growth. *Atherosclerosis.* 1987;68:51–58.
3. Hak AE, Pols HA, Visser TJ, Drexhage HA, Hofman A, Witteman JC. Subclinical hypothyroidism is an independent risk factor for atherosclerosis and myocardial infarction in elderly women: the Rotterdam Study. *Ann Intern Med.* 2000;132:270–278.
4. Lev-Ran A. Thyroid hormones and prevention of atherosclerotic heart disease: an old-new hypothesis. *Perspect Biol Med.* 1994;37:486–494.
5. Zhang J, Lazar MA. The mechanism of action of thyroid hormones. *Annu Rev Physiol.* 2000;62:439–466.
6. Funakoshi Y, Ichiki T, Ito K, Takeshita A. Induction of interleukin-6 expression by angiotensin II in rat vascular smooth muscle cells. *Hypertension.* 1999;34:118–125.
7. Funakoshi Y, Ichiki T, Takeda K, Tokunou T, Iino N, Takeshita A. Critical role of cAMP response element-binding protein (CREB) for

angiotensin II-induced hypertrophy of vascular smooth muscle cells. *J Biol Chem.* 2002;20:20.
8. Gonzalez GA, Yamamoto KK, Fischer WH, Karr D, Menzel P, Biggs W, 3rd, Vale WW, Montminy MR. A cluster of phosphorylation sites on the cyclic AMP-regulated nuclear factor CREB predicted by its sequence. *Nature.* 1989;337:749–752.
9. Shaywitz AJ, Greenberg ME. CREB: a stimulus-induced transcription factor activated by a diverse array of extracellular signals. *Annu Rev Biochem.* 1999;68:821–861.
10. Tokunou T, Shibata R, Kai H, Ichiki T, Morisaki T, Fukuyama K, Ono H, Iino N, Masuda S, Shimokawa H, Egashira K, Imaizumi T, Takeshita A. Apoptosis induced by inhibition of cyclic AMP response element-binding protein in vascular smooth muscle cells. *Circulation.* 2003;108: 1246–1252.
11. Mendez-Pertuz M, Sanchez-Pacheco A, Aranda A. The thyroid hormone receptor antagonizes CREB-mediated transcription. *Embo J.* 2003;22: 3102–3112.
12. Ichiki T, Tokunou T, Fukuyama K, Iino N, Masuda S, Takeshita A. Cyclic AMP response element-binding protein mediates reactive oxygen species-induced c-fos expression. *Hypertension.* 2003;42:177–183.
13. Ichiki T, Usui M, Kato M, Funakoshi Y, Ito K, Egashira K, Takeshita A. Downregulation of angiotensin II type 1 receptor gene transcription by nitric oxide. *Hypertension.* 1998;31:342–348.
14. Tokunou T, Ichiki T, Takeda K, Funakoshi Y, Iino N, Takeshita A. cAMP response element-binding protein mediates thrombin-induced proliferation of vascular smooth muscle cells. *Arterioscler Thromb Vasc Biol.* 2001;21:1764–1769.
15. Fukuyama K, Ichiki T, Takeda K, Tokunou T, Iino N, Masuda S, Ishibashi M, Egashira K, Shimokawa H, Hirano K, Kanaide H, Takeshita A. Downregulation of vascular angiotensin II type 1 receptor by thyroid hormone. *Hypertension.* 2003;41:598–603.
16. Dzau VJ. Mechanism of protective effects of ACE inhibition on coronary artery disease. *Eur Heart J.* 1998;19(Suppl J):J2–J6.
17. Goodfriend TL, Elliott ME, Catt KJ. Angiotensin receptors and their antagonists. *N Engl J Med.* 1996;334:1649–1654.
18. Geisterfer AA, Peach MJ, Owens GK. Angiotensin II induces hypertrophy, not hyperplasia, of cultured rat aortic smooth muscle cells. *Circ Res.* 1988;62:749–756.
19. Eguchi S, Dempsey PJ, Frank GD, Motley ED, Inagami T. Activation of MAPKs by angiotensin II in vascular smooth muscle cells. *Metalloprotease*-dependent EGF receptor activation is required for activation of ERK and p38 MAPK but not for JNK. *J Biol Chem.* 2001;276: 7957–7962.
20. Marchal S, Cassar-Malek I, Magaud JP, Rouault JP, Wrutniak C, Cabello G. Stimulation of avian myoblast differentiation by triiodothyronine: possible involvement of the cAMP pathway. *Experimental Cell Research.* 1995;220:1–10.
21. Lo MJ, Kau MM, Chen YH, Tsai SC, Chiao YC, Chen JJ, Liaw C, Lu CC, Lee BP, Chen SC, Fang VS, Ho LT, Wang PS. Acute effects of thyroid hormones on the production of adrenal cAMP and corticosterone in male rats. *Am J Physiol.* 1998;274:E238–E245.
22. Viswanathan M, Stromberg C, Seltzer A, Saavedra JM. Balloon angioplasty enhances the expression of angiotensin II AT1 receptors in neointima of rat aorta. *J Clin Invest.* 1992;90:1707–1712.
23. Kauffman RF, Bean JS, Zimmerman KM, Brown RF, Steinberg MI. Losartan, a nonpeptide angiotensin II (Ang II) receptor antagonist, inhibits neointima formation following balloon injury to rat carotid arteries. *Life Sci.* 1991;49:PL223–228.
24. Tagami T, Park Y, Jameson JL. Mechanisms that mediate negative regulation of the thyroid-stimulating hormone alpha gene by the thyroid hormone receptor. *J Biol Chem.* 1999;274:22345–22353.
25. Kakizawa T, Miyamoto T, Ichikawa K, Takeda T, Suzuki S, Mori J, Kumagai M, Yamashita K, Hashizume K. Silencing mediator for retinoid and thyroid hormone receptors interacts with octamer transcription factor-1 and acts as a transcriptional repressor. *J Biol Chem.* 2001;276: 9720–9725.
26. Lee SK, Kim JH, Lee YC, Cheong J, Lee JW. Silencing mediator of retinoic acid and thyroid hormone receptors, as a novel transcriptional corepressor molecule of activating protein-1, nuclear factor-kappaB, and serum response factor. *J Biol Chem.* 2000;275:12470–12474.
27. Hagiwara M, Brindle P, Harootunian A, Armstrong R, Rivier J, Vale W, Tsien R, Montminy MR. Coupling of hormonal stimulation and transcription via the cyclic AMP-responsive factor CREB is rate limited by nuclear entry of protein kinase A. *Mol Cell Biol.* 1993;13:4852–4859.
28. Mizuma H, Murakami M, Mori M. Thyroid hormone activation in human vascular smooth muscle cells: expression of type II iodothyronine deiodinase. *Circ Res.* 2001;88:313–318.

Original Article

Amlodipine-Induced Reduction of Oxidative Stress in the Brain Is Associated with Sympatho-Inhibitory Effects in Stroke-Prone Spontaneously Hypertensive Rats

Yoshitaka HIROOKA[1),*], Yoshikuni KIMURA[1),*], Masatsugu NOZOE[1)], Yoji SAGARA[1)], Koji ITO[1)], and Kenji SUNAGAWA[1)]

Amlodipine is a dihydropyridine calcium channel blocker that is widely used for the treatment of hypertensive patients and has an antioxidant effect on vessels *in vitro*. The aim of the present study was to examine whether treatment with amlodipine reduced oxidative stress in the brains of stroke-prone spontaneously hypertensive rats (SHRSP). The animals received amlodipine, nicardipine or hydralazine for 30 days in their drinking water. Levels of thiobarbituric acid-reactive substances (TBARS) in the brain (cortex, cerebellum, hypothalamus, and brainstem) were measured before and after each treatment. Systolic blood pressure decreased to similar levels in the amlodipine-, nicardipine-, and hydralazine-treated groups. Urinary norepinephrine excretion was significantly reduced in SHRSP after treatment with amlodipine, but not with nicardipine or hydralazine. Levels of TBARS in the cortex, cerebellum, hypothalamus, and brainstem were significantly higher in SHRSP than in Wistar-Kyoto rats (WKY), and were reduced in amlodipine-treated, but not in nicardipine- or hydralazine-treated, SHRSP. Electron spin resonance spectroscopy revealed increased levels of reactive oxygen species in the brains of SHRSP, which were reduced by treatment with amlodipine. Intracisternal infusion of amlodipine also reduced systolic blood pressure, urinary norepinephrine excretion, and the levels of TBARS in the brain. These results suggested that oxidative stress in the brain was enhanced in SHRSP compared with WKY rats. In addition, antihypertensive treatment with amlodipine reduced oxidative stress in all areas of the brain examined and decreased blood pressure without a reflex increase in sympathetic nerve activity in SHRSP. (*Hypertens Res* 2006; 29: 49–56)

Key Words: **blood pressure, heart rate, hypertension, oxidative stress, sympathetic nervous system**

Introduction

Amlodipine is a dihydropyridine calcium channel blocker that is widely used for the treatment of hypertension. Large clinical trials have confirmed its usefulness for preventing cardiovascular events by lowering blood pressure (*1*, *2*). Concern remains over the risk of cardiovascular events in patients

From the [1)]Department of Cardiovascular Medicine, Kyushu University Graduate School of Medical Sciences, Fukuoka, Japan.
*Each author contributed equally to this work.
This study was supported by Grants-in-Aid for Scientific Research from Japan Society for the Promotion of Science (C15590757, C17590745) of Japan, a Kimura Memorial Foundation Research Grant for 2003, a Grant from Pfizer Pharmaceutical Co. Inc., Japan, and a Grant from the Takeda Science Foundation. The electron spin resonance spectroscopy method was performed at the Kyushu University Station for Collaborative Research, Japan.
Address for Reprints: Yoshitaka Hirooka, M.D., Ph.D., Department of Cardiovascular Medicine, Kyushu University Graduate School of Medical Sciences, 3–1–1 Maidashi, Higashi-ku, Fukuoka 812–8582, Japan. E-mail: hyoshi@cardiol.med.kyushu-u.ac.jp
Received August 4, 2005; Accepted in revised form November 22, 2005.

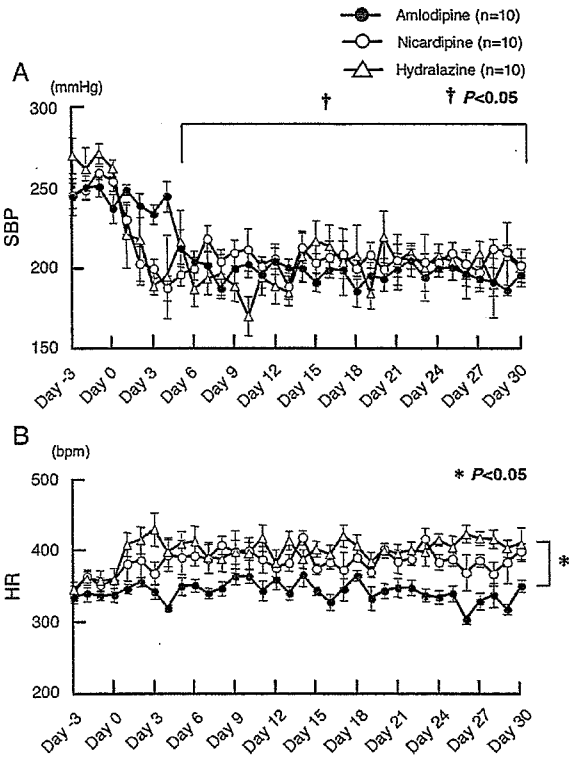

Fig. 1. *Time course of changes in systolic blood pressure (SBP) (A) and heart rate (HR) (B) induced by treatment with amlodipine, nicardipine and hydralazine.* †p < *0.05 compared with the baseline values.* *p < *0.05 for the difference between the two groups.*

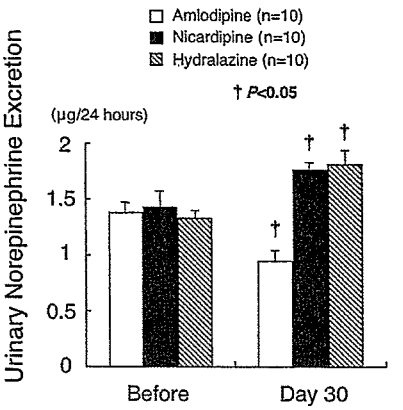

Fig. 2. *Urinary norepinephrine excretion for 24 h before and during the last day of (after) treatment with amlodipine, nicardipine and hydralazine.* †p < *0.05 compared with the values before treatment.*

with coronary artery disease, which is probably due to arterial baroreflex-mediated sympathoexcitation, particularly when short-acting calcium channel blockers are used (*3–5*). However, recent large clinical trials have indicated that this is not necessarily the case with long-acting dihydropyridine calcium channel blockers, such as amlodipine (*1, 2*). In addition, amlodipine has been demonstrated to have anti-atherosclerotic and anti-inflammatory effects in animals (*6–9*) and humans (*10*). The mechanisms involved are complex, and include an increase in nitric oxide production (*11*) and a decrease in oxidative stress (*12–14*).

The reported effects of amlodipine on sympathetic nerve activity vary among human studies, although it appears to lower blood pressure (*15–17*). Receptor binding sites for calcium channel blockers have been identified in the brain (*18–20*). In conscious spontaneously hypertensive rats (SHR), intracerebroventricular administration of nifedipine or amlodipine decreases blood pressure, heart rate and renal sympathetic nerve activity (*21, 22*). Furthermore, long-term i.v. infusion of nifedipine or amlodipine decreases these variables by inhibiting central sympathetic outflow (*21, 22*).

Increased nitric oxide levels and decreased oxidative stress in the brain, particularly in the brainstem, inhibit sympathetic nerve activity, thereby reducing blood pressure in stroke-prone SHR (SHRSP) (*23*). Increased oxidative stress is also involved in the pathogenesis of hypertension and hypertensive vascular lesion formation (*24*). We demonstrated previously that oxidative stress in the brain is increased in SHRSP, which is related to the increased sympathetic outflow in this model (*23*). Amlodipine reduces oxidative stress in the vasculature of hypertensive animals (*25*) and humans (*26, 27*). However, the antioxidant effect of amlodipine in the brain of hypertensive animals has not been reported previously. Therefore, the aim of the present study was to determine whether long-term oral treatment with amlodipine reduced oxidative stress in the brain of SHRSP, and to examine the associated changes in blood pressure, heart rate, and urinary norepinephrine excretion. For this purpose, we measured thiobarbituric acid-reactive substances (TBARS), which are the end products of lipid peroxidation and markers of oxidative stress (*23*). Electron spin resonance spectroscopy measurements (*23*) were also performed to analyze the production of reactive oxygen species.

Methods

General Preparation

This study was reviewed and approved by the Committee of Ethics of Animal Experiments, Kyushu University Graduate School of Medical Sciences, Japan. Male SHRSP/Izm (*14* weeks old; SLC Japan, Hamamatsu, Japan) were fed a standard diet with free access to drinking water. The animals received amlodipine in their drinking water at doses (3 or 10 mg/kg body weight/day) that were chosen based on previous studies (*12, 28–30*). Control groups were fed a standard diet

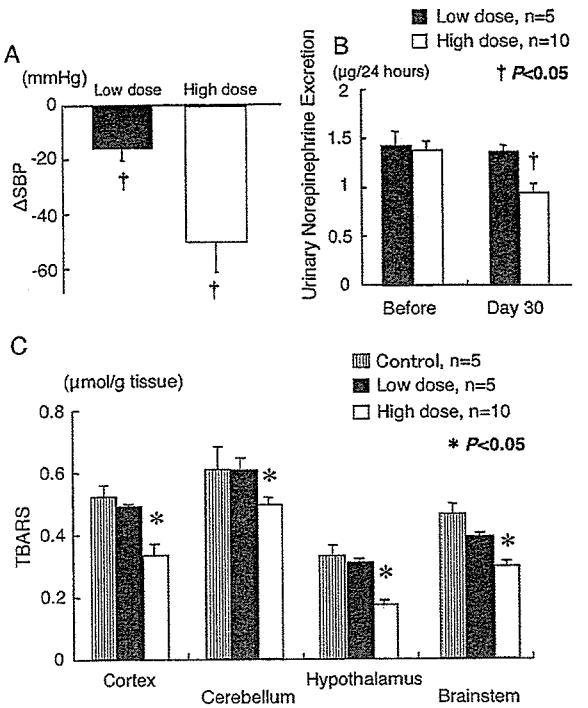

Fig. 3. *A: Amlodipine-induced changes in systolic blood pressure (ΔSBP) at doses of 3 or 10 mg/kg body weight/day. B: Urinary norepinephrine excretion for 24 h before and after amlodipine treatment. C: Levels of TBARS in the brain (cortex, cerebellum, hypothalamus and brainstem) in non-treated rats (control) and rats treated with amlodipine.* $^{\dagger}p < 0.05$ *compared with the baseline values.* $^{*}p < 0.05$ *for the difference between the two groups.*

and received nicardipine (10 mg/kg body weight/day) or hydralazine (20 mg/kg body weight/day) in their drinking water. The treatment commenced when the rats were 14 weeks of age and continued for 30 days. All drugs were dissolved in 45 ml of drinking water per day and, once this had been consumed, additional water was made available *ad libitum*.

Measurement of Blood Pressure, Heart Rate, and Urinary Norepinephrine Excretion

Systolic blood pressure and heart rate evaluated using the tail-cuff method were measured before and after treatment with amlodipine and the other drugs in SHRSP, as described previously (*31*). Urine was collected for 24 h in a metabolic cage. Urinary norepinephrine concentrations were measured before and after amlodipine, nicardipine or hydralazine treatment using high-performance liquid chromatography. Urinary norepinephrine excretion was calculated as a marker of sympathetic nerve activity (*23*, *31*).

Measurement of TBARS

Brain tissue was homogenized in 1.15% KCl (pH 7.4), and 0.4% sodium dodecyl sulfate, 7.5% acetic acid adjusted to pH 3.5 with NaOH and 0.3% TBA were added to the homogenate. The amounts of TBARS were determined by absorbance with a molecular extinction coefficient of 156,000 and expressed as μmol/g of wet weight tissue, as described previously (*23*, *32*).

Electron Spin Resonance Spectroscopy Measurements

Electron spin resonance spectroscopy measurements were performed at room temperature with an X-band (9.45-GHz) electron spin resonance spectrometer (JES-RE-1X; JEOL, Tokyo, Japan) at the following settings: microwave power of 10 mW, an external magnetic field range of 20 mT and a scan rate of 10 mT/min. The amounts of reactive oxygen species were quantified by monitoring the time-dependent decay of the amplitude of the electron spin resonance spectra elicited by the nitroxide radical 4-hydroxy-2,2,6,6-tetramethyl-piperidine-*N*-oxyl (hydroxy-TEMPO) as a spin probe. The tissue was homogenized in 50 mmol/l phosphate-buffered saline (PBS) containing the following protease inhibitors: leupeptin (10 g/ml), phenylmethylsulfonyl fluoride (100 g/ml), dithiothreitol (1 mmol/l) and trypsin inhibitor (10 μg/ml). The homogenate was mixed rapidly with hydroxy-TEMPO (0.1 mmol/l) in PBS and drawn into glass tubes. The electron spin resonance spectra were recorded for up to 10 min at 10-s intervals, as described previously (*23*, *32*, *33*).

Continuous Intracisternal (i.c.) Infusion Experiments with Amlodipine

The SHRSP were randomly divided into two groups, which received either artificial cerebrospinal fluid vehicle ($n=5$) or amlodipine (dissolved in artificial cerebrospinal fluid; 0.1 mg/kg body weight/day; $n=6$) by continuous i.c. infusion (0.25 μl/h) for 2 weeks *via* an osmotic minipump (Alzet model 1002; DURECT Corp., Cupertino, USA), as described previously (*34*, *35*). The treatment commenced when the rats were 14 weeks of age and continued for 2 weeks. Systolic blood pressure, heart rate, urinary norepinephrine concentrations, and levels of TBARS were measured before and after the infusion.

Drugs

Amlodipine was provided from Pfizer Japan Inc. Other drugs were purchased from Sigma Chemical Co. (St. Louis, USA).

Statistical Analysis

All values are expressed as the mean±SEM). Two-way anal-

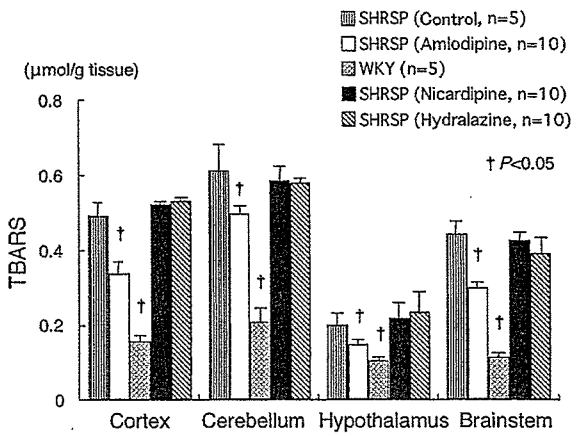

Fig. 4. *Levels of TBARS in the brain (cortex, cerebellum, hypothalamus and brainstem) in non-treated rats (control) and rats treated with amlodipine, nicardipine or hydralazine.* †p *< 0.05 compared with the values for non-treated rats.*

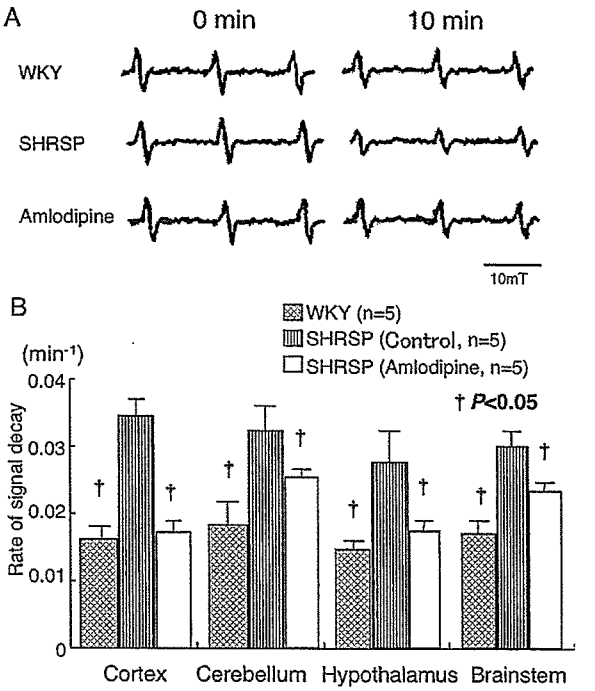

Fig. 5. *Electron spin resonance analysis of hydroxy-TEMPO in the tissues. A: Sequential sample of electron spin resonance spectra of hydroxy-TEMPO in brainstem tissues from SHRSP (middle spectra), SHRSP treated with amlodipine (lower spectra) and WKY rats (upper spectra). B: Summary data for the signal decay rate in the brain (cortex, cerebellum, hypothalamus and brainstem) in WKY rats, SHRSP and SHRSP treated with amlodipine.* †p *< 0.05 compared with the values for non-treated SHRSP (control).*

ysis of variance (ANOVA) was used to compare the systolic blood pressure and heart rate between the amlodipine-treated and other groups. Comparisons between any two mean values were performed using Bonferroni's correction for multiple comparisons. ANOVA was used to compare the amounts of TBARS and the electron spin resonance signal-decay rates in non-treated SHRSP and other rats in conjunction with a *post hoc* test using Scheffe's correction. A paired *t*-test was performed to compare the urinary norepinephrine excretion before and after treatment. Differences were considered to be statistically significant when p was less than 0.05.

Results

Effects of Amlodipine on Blood Pressure, Heart Rate, and Urinary Norepinephrine Excretion

Systolic blood pressure was reduced to similar levels in the high-dose amlodipine- and hydralazine-treated groups; the values for amlodipine, nicardipine and hydralazine were -40 ± 12, -45 ± 7 and -43 ± 8 mmHg, respectively ($n=10$ for each; Fig. 1A). By contrast, heart rate was not significantly affected by amlodipine treatment, but was increased by nicardipine and hydralazine treatment (Fig. 1B). Urinary norepinephrine excretion was significantly higher in SHRSP than in WKY rats, with values of 1.38 ± 0.10 and 0.76 ± 0.03 μg/day, respectively ($n=6$ for both; $p<0.05$). Furthermore, urinary norepinephrine excretion was decreased in SHRSP after amlodipine treatment, but was significantly increased after nicardipine or hydralazine treatment; the values were 1.37 ± 0.15 *vs.* 0.87 ± 0.10 μg/day, 1.45 ± 0.17 *vs.* 1.68 ± 0.06 μg/day and 1.33 ± 0.08 *vs.* 1.77 ± 0.14 μg/day for amlodipine, nicardipine, and hydralazine, respectively ($n=10$; $p<0.05$; Fig. 2). Treatment with a high dose of amlodipine decreased the systolic blood pressure to a greater extent than treatment with a low dose, with values of -40 ± 12 and -18 ± 7 mmHg, respectively ($p<0.05$; Fig. 3A). Urinary norepinephrine excretion was not significantly different before and after treatment with a low dose of amlodipine (1.44 ± 0.25 *vs.* 1.38 ± 0.15 μg/day; Fig. 3B).

Reactive Oxygen Species Generation in the Brain

Levels of TBARS in the cortex, cerebellum, hypothalamus and brainstem were significantly higher in SHRSP than in WKY rats ($p<0.05$; $n=5$ for both). Furthermore, levels of TBARS in each area of the brain examined were significantly reduced in the high-dose amlodipine-treated, but not in the nicardipine- or hydralazine-treated, SHRSP ($p<0.05$; $n=10$ for each; Fig. 4). The levels of TBARS in all areas of the brain examined were not significantly altered in the low-dose amlodipine-treated SHRSP (Fig. 3C). The intensity of electron spin resonance signals in each area of the brain decreased more rapidly in SHRSP than in WKY rats (Fig. 5A). The rates

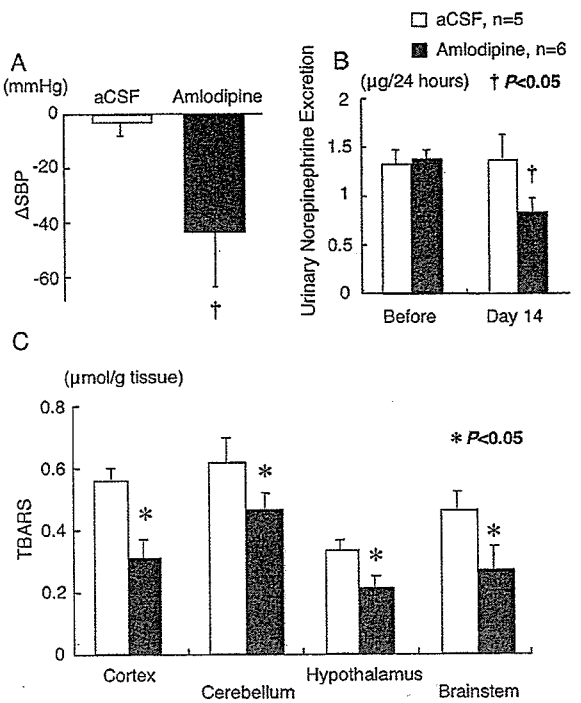

Fig. 6. *A: Changes in systolic blood pressure (ΔSBP) caused by continuous i.c. infusion with amlodipine or artificial cerebrospinal fluid (aCSF) for 2 weeks. B: Urinary norepinephrine excretion for 24 h at days 0 and 14. C: Levels of TBARS in the brain (cortex, cerebellum, hypothalamus and brainstem) in non-treated rats and rats treated with amlodipine at days 0 and 14.* †$p<0.05$ *compared with the values before treatment.* *$p<0.05$ *for the difference between the two groups.*

of signal decay in the cortex, cerebellum, hypothalamus and brainstem, calculated from the slopes of the lines, were significantly higher in SHRSP than in WKY rats ($p<0.05$; $n=5$ for each; Fig. 5B). Furthermore, the rates of signal decay in these areas of the brain were significantly reduced in amlodipine-treated SHRSP ($p<0.05$; $n=5$ for each; Fig. 5B).

Effect of Continuous i.c. Infusion with Amlodipine

The changes in systolic blood pressure after the i.c. infusion of amlodipine for 2 weeks are shown in Fig. 6A. The changes in systolic blood pressure were significantly greater after treatment with amlodipine (-43 ± 22 mmHg; $n=6$) than after treatment with artificial cerebrospinal fluid (-3 ± 12 mmHg; $n=5$; $p<0.05$). Figure 6B shows that urinary norepinephrine excretion was significantly decreased in SHRSP after treatment with amlodipine (1.45 ± 0.10 *vs.* 0.67 ± 0.11; $n=6$; $p<0.05$), but was not significantly altered by treatment with artificial cerebrospinal fluid (1.42 ± 0.08 *vs.* 1.48 ± 0.20 μg/day; $n=5$). The levels of TBARS in all areas of the brain were significantly reduced in amlodipine- but not artificial cerebrospinal fluid-treated SHRSP ($n=6$ and 5, respectively; $p<0.05$; Fig. 6C).

Discussion

The major findings of the present study were that oral treatment with amlodipine did not induce reflex tachycardia and reduced sympathetic nerve activity. In addition, amlodipine decreased oxidative stress in the brains of SHRSP, as evaluated by the measurement of levels of TBARS. By contrast, treatment with hydralazine induced sympathoexcitation and reflex tachycardia, but did not alter levels of TBARS. Nicardipine, which is another calcium channel blocker, also induced sympathoexcitation and reflex tachycardia, but did not alter TBARS levels. The electron spin resonance spectroscopy results indicated increased reactive oxygen species production in SHRSP, which was attenuated after treatment with amlodipine. These findings suggest that long-term antihypertensive treatment with amlodipine does not cause reflex-induced sympathoexcitation and reduces the increased oxidative stress in the brains of SHRSP. In particular, the decreased oxidative stress levels in the brainstem and hypothalamus might be related to a decrease in sympathetic nerve activity.

A gradual decrease in blood pressure was observed over time in rats treated with amlodipine compared with those treated with hydralazine or nicardipine, due to differences in the pharmacokinetic profiles, plasma concentrations and lipophilicities of the drugs (*16*, *21–33*, *36*). Disrupted tight junctions caused by endothelial dysfunction are responsible for the increased permeability of tracers through the blood–brain barrier in chronic hypertension (*37*). L-type voltage-gated calcium channels in the central nervous system and dihydropyridines act on these receptors (*19*, *20*, *38–40*). Thus, it is possible that lipophilic dihydropyridines (such as nifedipine and amlodipine) are able to cross the blood–brain barrier in chronic hypertension (*21*, *22*) and reduce the generation of reactive oxygen species (*41–43*). However, this might not occur with all calcium channel blockers, as nicardipine did not reduce the generation of reactive oxygen species.

We believe that treatment with the lower dose of amlodipine in our study was not sufficient to reduce the oxidative stress in the brain. In addition, urinary norepinephrine excretion was not altered. By contrast, treatment with the higher dose of amlodipine induced a greater reduction in blood pressure, which was associated with a decrease in urinary norepinephrine excretion. Oxidative stress in the brain was also reduced. A greater reduction in blood pressure is thought to elicit a greater reflex increase in sympathetic nerve activity. Thus, these results suggest that treatment with amlodipine, at a dose that is sufficient to decrease blood pressure, reduces oxidative stress in the brain in association with sympathoinhibition.

Brain cell membranes contain a high concentration of polyunsaturated fatty acids (*44*). These are targets of free radicals, which cause chain reactions of lipid peroxidation (*45*). TBARS, which are the end products of lipid peroxidation and markers of oxidative stress, were increased in the brain of SHRSP (*23*). In the present study, we examined levels of TBARS in the cortex, cerebellum, hypothalamus and brainstem, and found that they were all increased in SHRSP compared with WKY rats. This was consistent with the results of our recent study, in which we compared levels of TBARS in the whole brain, the rostral ventrolateral medulla and the nucleus tractus solitarius of SHRSP and WKY rats (*46*). These areas are important for autonomic cardiovascular regulation (*47*, *48*). The electron spin resonance spectroscopy results further support the theory that there is increased generation of reactive oxygen species in the brain of SHRSP compared with WKY rats. Moreover, this increase was attenuated by amlodipine.

Although variable effects on the sympathetic nervous system have been reported in clinical studies in humans (*16–18*, *26*), lipophilic dihydropyridines (such as nifedipine and amlodipine) are believed to have sympatho-inhibitory and depressor effects through central nervous system mechanisms in SHR (*21*, *22*). During long-term i.v. infusion, nifedipine and amlodipine cross the blood–brain barrier and, thereafter, inhibit sympathetic nerve activity and reduce blood pressure (*21*, *22*). Furthermore, intracerebroventricular injection of these calcium channel blockers reduces blood pressure, heart rate, and renal sympathetic nerve activity (*21*, *22*). In addition, direct microinjection of calcium channel blockers into the nucleus tractus solitarius of the brainstem reduces blood pressure and heart rate *via* the inhibition of central sympathetic outflow (*49*). In the present study, amlodipine administered by i.c. infusion decreased blood pressure, urinary norepinephrine excretion and oxidative stress in the brain, further supporting the idea that it elicits these effects by acting on the central nervous system. There were no effects on blood pressure and heart rate when we intravenously administered the same concentration of amlodipine as used for the intracisternal infusion for 1 h (data not shown). Although the site of the sympatho-inhibitory actions of amlodipine in the central nervous system is not known, we consider the hypothalamus and brainstem to be likely candidates. In conjunction with the decrease in reactive oxygen species generation, an increase in endothelial nitric oxide synthase activity might be related to the decrease in oxidative stress and central sympathetic outflow in SHRSP (*31*, *50–52*). In fact, amlodipine enhances endothelial nitric oxide synthase activity (*53*), although we did not address this issue in the present study. Increased nitric oxide production in the brainstem also produces a decrease in central sympathetic outflow (*50–52*). Amlodipine may reduce reactive oxygen species by upregulating Cu/Zn superoxide dismutase in SHRSP (*54*).

Several previous studies have suggested that the generation of reactive oxygen species leads to hypertensive vascular-lesion formation (*55–60*). Therefore, therapies aimed at reducing the generation of reactive oxygen species might be useful for hypertensive patients. In particular, the brain is the organ that is most affected by hypertension (*55*). In the present study, we demonstrated that oral treatment with amlodipine reduced oxidative stress in the cortex and cerebellum, as well as the hypothalamus and brainstem; the effects on the latter might help reduce sympathetic nerve activity, thereby preventing cardiovascular events, whereas the effects on the former might help to protect brain function. Hypertension accelerates age-related organ damage, which is also associated with sympathetic dysregulation (*55*, *56*). In addition, dementia might be related to hypertension (*60*). Further studies will be required to examine how treatment with amlodipine leads to the reduction of reactive oxygen species. It is possible that long-term treatment for hypertension, as well as the reduction of oxidative stress in the brain, will result in a better quality of life for patients.

We cannot exclude the possibility that amlodipine might act on the peripheral sympathetic nervous system, thereby inhibiting the sympathetic nerve activity. In particular, amlodipine has been shown to block both N-type Ca^{2+} channels and L-type Ca^{2+} channels (*61*, *62*), although the extent of these actions has not been clarified *in vivo*. Nicardipine has also been reported to exhibit this blocking activity (*62*). However, we found different results between amlodipine and nicardipine. Furthermore, the present study does not provide direct evidence that an increase in oxidative stress in the brain inhibits sympathetic nerve activity, thereby reducing blood pressure. Thus, it remains unknown whether the decrease in reactive oxygen species in the brain is a cause or an effect of sympatho-inhibition or blood pressure reduction from the results of the present study. The reduction of blood pressure itself, however, did not decrease oxidative stress in the brain when we administered hydralazine or nicardipine. Finally, we used a high dose of amlodipine in the present study. Although this dose of amlodipine (10 mg/kg/day) has been used in other experimental studies (*12*, *28–30*), it did require us to adjust the level of blood pressure reduction among the treatments.

In conclusion, the results of the present study suggest that long-term treatment with amlodipine decreases the generation of reactive oxygen species in several areas of the brain, including the hypothalamus and brainstem. This mechanism might be associated with a reduction in sympathetic nerve activity in SHRSP.

References

1. The ALLHAT Officers and Coordinators for the ALLHAT Collaborative Research Group: Major outcomes in high-risk hypertensive patients randomized to angiotensin-converting enzyme inhibitor or calcium channel blocker *vs* diuretic. The Antihypertensive and Lipid-Lowering Treatment to Prevent Heart Attack Trial (ALLHAT). *JAMA* 2002; **288**: 2981–2997.

2. Julius S, Kjeldsen SE, Weber M, *et al*: Outcomes in hypertensive patients at high cardiovascular risk treated with regimens based on valsartan or amlodipine: the VALUE randomised trial. *Lancet* 2004; **363**: 2022–2031.
3. Furberg CD, Psaty BM, Meyer JV: Nifedipine: dose-related increase in mortality in patients with coronary heart disease. *Circulation* 1995; **92**: 1325–1331.
4. Pahor M, Applegate WB, Williamson JD, *et al*: Health outcomes associated with calcium antagonists compared with other first-line antihypertensive therapies: a meta-analysis of randomized controlled trials. *Lancet* 2000; **356**: 1949–1954.
5. Opie LH, Yasuf S, Küber W: Current status of safety and efficacy of calcium channel blockers in cardiovascular diseases: a critical analysis based on 100 studies. *Prog Cardiovasc Dis* 2000; **43**: 171–196.
6. Chen L, Haught WH, Yang B, Saldeen TG, Parathasarathy S, Mehta JL: Preservation of endogenous antioxidant activity and inhibition of lipid peroxidation as common mechanisms of antiatherosclerotic effects of vitamin E, lovastatin and amlodipine. *J Am Coll Cardiol* 1997; **30**: 569–575.
7. Kataoka C, Egashira K, Ishibashi M, *et al*: Novel antiinflammatory actions of amlodipine in a rat model of arteriosclerosis induced by long-term inhibition of nitric oxide synthesis. *Am J Physiol Heart Circ Physiol* 2004; **286**: H768–H774.
8. Gerzanich V, Ivanova S, van der Heijden MS, Zhou H, Simard JM: Trans-cellular proliferating cell nuclear antigen gene activation in cerebral vascular smooth muscle by endothelial oxidative injury *in vivo*. *Arterioscler Thromb Vasc Biol* 2003; **23**: 2048–2054.
9. Blezer ELA, Nicolay K, Goldschmeding R, Koomans HA, Joles JA: Reduction of cerebral injury in stroke-prone spontaneously hypertensive rats by amlodipine. *Eur J Pharmacol* 2002; **444**: 75–81.
10. Pitt B, Byington RP, Furberg CD, *et al*, PREVENT Investigators: Effect of amlodipine on the progression of atherosclerosis and the occurrence of clinical events. *Circulation* 2000; **102**: 1503–1510.
11. Zhang X, Hintze TH: Amlodipine releases nitric oxide from canine coronary microvessels: an unexpected mechanism of action of a calcium channel-blocking agent. *Circulation* 1998; **97**: 576–580.
12. Zhou M-S, Jaimes EA, Raij L: Inhibition of oxidative stress and improvement of endothelial function by amlodipine in angiotensin II-infused rats. *Am J Hypertens* 2004; **17**: 167–171.
13. Mason RP, Walter MF, Trumbore MW, Olmstead EG Jr, Mason PE: Membrane antioxidant effects of the charged dihydropyridine calcium antagonist amlodipine. *J Mol Cell Cardiol* 1999; **31**: 275–281.
14. Yamagata K, Ichinose S, Tagami M: Amlodipine and carvedilol prevent cytotoxicity in cortical neurons isolated from stroke-prone spontaneously hypertensive rats. *Hypertens Res* 2004; **27**: 271–282.
15. Binggeli C, Corti R, Sudano I, Luscher TF, Noll G: Effects of chronic calcium channel blockade on sympathetic nerve activity in hypertension. *Hypertension* 2002; **39**: 892–896.
16. Fogari R, Zoppi A, Corradi L, Preti P, Malalamani GD, Mugellini A: Effects of different dihydropyridine calcium antagonists on plasma norepinephrine in essential hypertension. *J Hypertens* 2000; **18**: 1871–1875.
17. Hamada T, Watanabe M, Kaneda T, *et al*: Evaluation of changes in sympathetic nerve activity and heart rate in essential hypertensive patients induced by amlodipine and nifedipine. *J Hypertens* 1998; **16**: 111–118.
18. Ishimitsu T, Kobayashi T, Honda T, *et al*: Protective effects of an angiotensin II receptor blocker and a long-acting calcium channel blocker against cardiovascular organ injuries in hypertensive patients. *Hypertens Res* 2005; **28**: 351–359.
19. Soong TW, Stea A, Hodson CD, Dubel SJ, Vincent SR, Snutch TP: Structure and functional expression of a member of the low voltage-activated calcium channel family. *Science* 1993; **260**: 1133–1136.
20. Miller RJ: Multiple calcium channels and neuronal function. *Science* 1987; **235**: 46–52.
21. Murzenok PP, Huang BS, Leenen FHH: Sympatho-inhibition by central and peripheral infusion of nifedipine in spontaneously hypertensive rats. *Hypertension* 2000; **35**: 631–636.
22. Huang BS, Leenen FHH: Sympathoinhibitory and depressor effects of amlodipine in spontaneously hypertensive rats. *J Cardiovasc Pharmacol* 2003; **42**: 153–160.
23. Kishi T, Hirooka Y, Kimura Y, Ito K, Shimokawa H, Takeshita A: Increased reactive oxygen species in rostral ventrolateral medulla contribute to neural mechanisms of hypertension in stroke-prone spontaneously hypertensive rats. *Circulation* 2004; **109**: 2357–2362.
24. Touyz RM: Reactive oxygen species, vascular oxidative stress, and redox signaling in hypertension. *Hypertension* 2004; **44**: 248–252.
25. Ganafa AA, Walton M, Eatman D, Abukhalaf IK, Bayorh MA: Amlodipine attenuates oxidative stress-induced hypertension. *Am J Hypertens* 2004; **17**: 743–748.
26. De Champlain J, Karas M, Nguyen P, *et al*: Different effects of nifedipine and amlodipine on circulating catecholamine levels in essential hypertensive patients. *J Hypertens* 1998; **16**: 1357–1369.
27. Taddei S, Virdis A, Ghiadoni L, *et al*: Calcium antagonist treatment by lercanidipine prevents hyperpolarization in essential hypertension. *Hypertension* 2003; **41**: 950–955.
28. Yavuz DG, Tugler S, Koçak H, Ozener C, Akoglu E, Akalin S: Angiotensin converting enzyme inhibition and calcium channel blockage improves cyclosporine induced glucose intolerance in rats. *Transplant Proc* 2004; **36**: 171–174.
29. Toblli JE, Stella I, Mazza ON, Fender L, Inserra F: Different effect of losartan and amlodipine on penile structure in male spontaneously hypertensive rats. *Am J Nephrol* 2004; **24**: 614–623.
30. Toba H, Nakagawa Y, Miki S, *et al*: Calcium channel blockades exhibit anti-inflammatory and antioxidative effects by augmentation of endothelial nitric oxide synthase and the inhibition of angiotensin converting enzyme in the N^G-nitro-L-arginine methyl ester-induced hypertensive rat aorta: vasoprotective effects beyond the blood pressure lowering effects of amlodipine and manidipine. *Hypertens Res* 2005; **28**: 689–700.
31. Kishi T, Hirooka Y, Mukai Y, Shimokawa H, Takeshita A: Atorvastatin causes depressor and sympatho-inhibitory

effects with upregulation of nitric oxide synthases in stroke-prone spontaneously hypertensive rats. *J Hypertens* 2003; **21**: 379–386.
32. Ide T, Tsutsui H, Kinugawa S, *et al*: Mitochondrial electron transport complex I is a potential source of oxygen free radicals in the failing myocardium. *Circ Res* 1999; **85**: 357–363.
33. Ide T, Tsutsui H, Kinugawa S, *et al*: Direct evidence for increased hydroxyradicals originating from superoxide in the failing myocardium. *Circ Res* 2000; **86**: 152–157.
34. Ito K, Hirooka Y, Kishi T, *et al*: Rho/Rho-kinase pathway in the brainstem contributes to hypertension caused by chronic nitric oxide synthase inhibition. *Hypertension* 2004; **43**: 156–162.
35. Kimura Y, Hirooka Y, Sagara Y, *et al*: Overexpression of inducible nitric oxide synthase in rostral ventrolateral medulla causes hypertension and sympathoexcitation *via* an increase in oxidative stress. *Circ Res* 2005; **96**: 252–260.
36. Sugawara H, Tobise K, Kikuchi K: Antioxidant effects of calcium antagonists on rat myocardial membrane lipid peroxidation. *Hypertens Res* 1996; **19**: 223–228.
37. Lippoldt A, Kneisel U, Liebner S, *et al*: Structural alterations of tight junctions are associated with loss of polarity in stroke-prone spontaneously hypertensive rat blood–brain barrier endothelial cells. *Brain Res* 2000; **885**: 251–261.
38. Lu C, Chan SL, Mattson MP: The lipid peroxidation product 4-hydroxynoneal facilitates opening of voltage-dependent Ca^{2+} channels in neurons by increasing protein tyrosine phosphorylation. *J Biol Chem* 2002; **277**: 24368–24375.
39. Tseng W-P, Lin-Shiau S-Y: Neuronal death signaling by β-bungarotoxin through the activation of the *N*-methyl-D-aspartate (NMDA) receptor and L-type calcium channel. *Biochem Pharmacol* 2003; **65**: 131–142.
40. Wang R-M, Zhang Q-G, Zhang G-Y: Activation of ERK5 is mediated by *N*-methyl-D-aspartate receptor and L-type voltage-gated calcium channel *via* Src involving oxidative stress after cerebral ischemia in rat hippocampus. *Neurosci Lett* 2004; **357**: 13–16.
41. Fukuo K, Yang J, Yasuda O, *et al*: Nifedipine indirectly upregulates superoxide dismutase expression in endothelial cells *via* vascular smooth muscle cell–dependent pathways. *Circulation* 2002; **106**: 356–361.
42. Napoli C, Salomone S, Godfraind T, *et al*: 1,4-Dihydropyridine calcium channel blockers inhibit plasma and LDL oxidation and formation of oxidation-specific epitopes in the arterial wall and prolong survival in stroke-prone spontaneously hypertensive rats. *Stroke* 1999; **30**: 1907–1915.
43. Hou X, Gobeil F, Marrache AM, *et al*: Increased platelet-activating factor-induced periventricular brain microvascular constriction associated with immaturity. *Am J Physiol Regul Integr Comp Physiol* 2003; **284**: 928–935.
44. Kikugawa K, Kojima T, Yamaki S, Kosugi H: Interpretation of the thiobarbituric acid reactivity of rat liver and brain homogenates in the presence of ferric ion and ethylenediaminetetraacetic acid. *Anal Biochem* 1992; **202**: 249–255.
45. Ohtsuki T, Matsumoto M, Suzuki K, Taniguchi N, Kamada T: Mitochondrial lipid peroxidation and superoxide dismutase in rat hypertensive target organs. *Am J Physiol* 1995; **268**: H1418–H1421.
46. Kishi T, Hirooka Y, Ito K, Sakai K, Shimokawa H, Takeshita A: Cardiovascular effects of overexpression of endothelial nitric oxide synthase in the rostral ventrolateral medulla in stroke-prone spontaneously hypertensive rats. *Hypertension* 2002; **39**: 264–268.
47. Dampney RAL: Functional organization of central pathways regulating the cardiovascular system. *Physiol Rev* 1994; **74**: 323–364.
48. Pilowsky PM, Goodchild AK: Baroreceptor reflex pathways and neurotransmitters: 10 years on. *J Hypertens* 2002; **20**: 1675–1688.
49. Higuchi S, Takeshita A, Ito N, Imaizumi T, Matsuguchi H, Nakamura M: Arterial pressure and heart rate responses to calcium channel blockers administered in the brainstem in rats. *Circ Res* 1985; **57**: 244–251.
50. Zanzinger J: Mechanisms of action of nitric oxide in the brain stem. *Auton Neurosci* 2002; **98**: 24–27.
51. Patel KP, Li Y-F, Hirooka Y: Role of nitric oxide in central sympathetic outflow. *Exp Biol Med* 2001; **226**: 814–824.
52. Hirooka Y, Sakai K, Kishi T, Ito K, Shimokawa H, Takeshita A: Enhanced depressor response to endothelial nitric oxide synthase gene transfer into the nucleus tractus solitarii of spontaneously hypertensive rats. *Hypertens Res* 2003; **26**: 325–331.
53. Berkels R, Taubert D, Bartels H, Bretenbach T, Klaus W, Roesen R: Amlodipine increases endothelial nitric oxide by dual mechanisms. *Pharmacology* 2004; **70**: 39–45.
54. Umemoto S, Tanaka M, Kawahara S, *et al*: Calcium antagonist reduces oxidative stress by upregulating Cu/Zn superoxide dismutase in stroke-prone spontaneously hypertensive rats. *Hypertens Res* 2004; **27**: 877–885.
55. Kerr S, Brosnan J, McIntyre M, Reid JL, Domniczak AF, Hamilton CA: Superoxide anion production is increased in a model of genetic hypertension. *Hypertension* 1999; **33**: 1353–1358.
56. Kimoto-Kinoshita S, Nishida S, Tomura TT: Age-related change of anti-oxidant capacities in the cerebral cortex and hippocampus of stroke-prone spontaneously hypertensive rats. *Neurosci Lett* 1999; **273**: 41–44.
57. Wilson SK: Role of oxygen-derived free radicals in acute angiotensin II-induced hypertensive vascular disease in the rat. *Circ Res* 1990; **66**: 722–734.
58. Zhang XM, Ellis EF: Superoxide dismutase reduces permeability and edema induced by hypertension in rats. *Am J Physiol* 1990; **259**: H497–H503.
59. Grunfeld S, Hamilton CA, Mesaros S, *et al*: Role of superoxide in the depressed nitric oxide production by the endothelium of genetically hypertensive rats. *Hypertension* 1995; **26**: 854–857.
60. Spence JD: Preventing dementia by treating hypertension and preventing stroke. *Hypertension* 2004; **44**: 20–21.
61. Furukawa T, Nukada T, Suzuki K, *et al*: Voltage and pH dependent block of cloned N-type Ca^{2+} channels by amlodipine. *Br J Pharmacol* 1997; **121**: 1136–1140.
62. Uneyama H, Uchida H, Konda T, Yoshimoto R, Akaike N: Selectivity of dihydropyridines for cardiac L-type and sympathetic N-type Ca^{2+} channels. *Eur J Pharmacol* 1999; **373**: 93–100.

Original Article

cAMP-Response Element-Binding Protein Mediates Tumor Necrosis Factor-α-Induced Vascular Cell Adhesion Molecule-1 Expression in Endothelial Cells

Hiroki ONO[1], Toshihiro ICHIKI[1], Hideki OHTSUBO[1], Kae FUKUYAMA[1], Ikuyo IMAYAMA[1], Naoko IINO[1], Satoko MASUDA[1], Yasuko HASHIGUCHI[1], Akira TAKESHITA[1], and Kenji SUNAGAWA[1]

Hypertension causes endothelial dysfunction, which plays an important role in atherogenesis. The vascular cell adhesion molecule-1 (VCAM-1) contributes to atherosclerotic lesion formation by recruiting leukocytes from blood into tissues. Tumor necrosis factor-α (TNFα) induces endothelial dysfunction and VCAM-1 expression in endothelial cells (ECs). We examined whether the cAMP-response element binding protein (CREB), a transcription factor that mediates cytokine expression and vascular remodeling, is involved in TNFα-induced VCAM-1 expression. TNFα induced phosphorylation of CREB with a peak at 15 min of stimulation in a dose-dependent manner in bovine aortic ECs. Pharmacological inhibition of p38 mitogen-activated protein kinase (p38-MAPK) inhibited TNFα-induced CREB phosphorylation. Adenovirus-mediated overexpression of a dominant-negative form of CREB suppressed TNFα-induced VCAM-1 and *c-fos* expression. Although activating protein 1 DNA binding activity was attenuated by overexpression of dominant negative CREB, nuclear factor-κB activity was not affected. Our results suggest that the p38-MAPK/CREB pathway plays a critical role in TNFα-induced VCAM-1 expression in vascular endothelial cells. The p38-MAPK/CREB pathway may be a novel therapeutic target for the treatment of atherosclerosis. (*Hypertens Res* 2006; 29: 39–47)

Key Words: **endothelial factors, cytokine, gene expression, mitogen-activated protein kinase, signal transduction**

Introduction

The initial step of atherogenesis involves attachment of mononuclear leukocytes to endothelial cells (ECs) and migration into the subendothelial space (*1*). Adhesion molecules expressed in ECs play an important role in the attachment of mononuclear leukocytes. Various cardiovascular risk factors including hypertension have been shown to increase the levels of soluble adhesion molecules, such as the vascular cell adhesion molecule-1 (VCAM-1), intercellular adhesion molecule-1 (ICAM-1) and E-selectin (*2–4*). Carotid intima-media thickness has been positively correlated with the plasma level of circulating soluble cellular adhesion molecules (*5*). VCAM-1 is expressed in ECs predisposed to atherosclerotic lesion formation (*6*) and contributes to recruitment of mono-

From the [1]Department of Cardiovascular Medicine, Kyushu University Graduate School of Medical Sciences, Fukuoka, Japan.

This study was supported in part by grants from the Takeda Medical Research Foundation and a Grant-in-Aid for Scientific Research from the Ministry of Education, Culture, Sports, Science and Technology of Japan (14570673).

Address for Reprints: Toshihiro Ichiki, M.D., Department of Cardiovascular Medicine, Kyushu University Graduate School of Medical Sciences, 3–1–1 Maidashi, Higashi-ku, Fukuoka 812–8582, Japan. E-mail: ichiki@cardiol.med.kyushu-u.ac.jp

Received June 16, 2005; Accepted in revised form November 7, 2005.

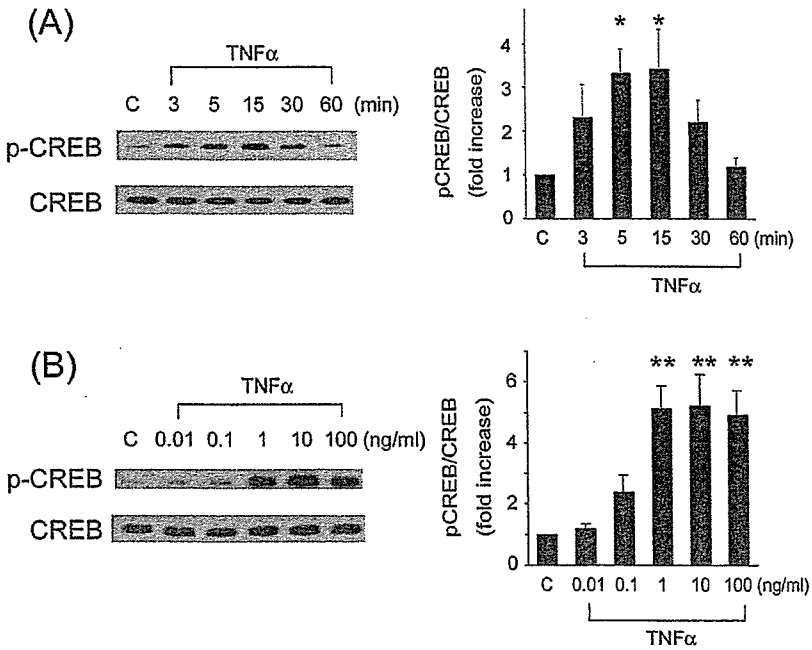

Fig. 1. *CREB is phosphorylated at Ser133 by TNFα. A: Bovine ECs were stimulated with TNFα (1 ng/ml) for varying periods indicated in the figure* (n=*4). B: Bovine ECs were stimulated with TNFα for 15 min at concentrations varying from 0.01 to 100 ng/ml* (n=*4). Phosphorylation of CREB was detected by Western blot analysis using a phospho-specific CREB antibody. The density of the specific band was scanned and quantified with an imaging analyzer. The ratio of phosphorylated CREB to total CREB in TNFα-stimulated cells is shown as the relative fold increase compared with that in unstimulated cells. The values are expressed as the mean±SEM.* *p < *0.05,* **p < *0.01* vs. *the control.*

nuclear leukocytes by binding to α4β1-integrin expressed on leukocytes (*7*).

Tumor necrosis factor-α (TNFα) is a multifunctional cytokine produced by activated macrophages, monocytes and lymphocytes. The vascular EC is an important target of TNFα (*1, 8*). A previous study demonstrated that *in vivo* blockade of TNFα accelerated functional endothelial recovery after angioplasty (*9*). TNFα is known to modulate the expression of many genes involved in cytoadhesion, thrombosis, and inflammatory response in ECs, resulting in the acquisition of new functional capacities leading to atherosclerosis (*10*). VCAM-1 is one of the molecules induced by TNFα (*11*).

cAMP-response element (CRE)-binding protein (CREB) is a 43 kD nuclear transcription factor belonging to the CREB/ATF family (*12, 13*). Phosphorylation of the serine residue at 133 (Ser133), which recruits a transcriptional coactivator, CREB-binding protein (CBP) or p300, is necessary for transcriptional activation. The phosphorylation of Ser133 is mediated by a variety of protein kinase pathways, such as 1) protein kinase A (PKA), 2) Ca^{2+}/calmodulin-dependent protein kinase (CaMK) II (*14*), 3) extracellular signal-regulated protein kinase (ERK) (*15, 16*), 4) p38 mitogen-activated protein kinase (p38-MAPK) (*17*), and 5) phosphatidylinositol 3-kinase (PI3-K) (*18*).

Although TNFα is known to activate transcription factors such as activating protein 1 (AP-1) and nuclear factor-κB (NF-κB) (*19, 20*), it has not been examined whether TNFα activates CREB in ECs. We investigated whether CREB is activated by TNFα in bovine ECs. We report in the present study that TNFα phosphorylated CREB through p38-MAPK and CREB mediated TNFα-induced VCAM-1 expression.

Methods

Materials

Dulbecco's modified Eagle's medium (DMEM) was purchased from GIBCO BRL (Gaithersburg, USA). Fetal bovine serum (FBS) was purchased from BioWhittaker (Walkersville, USA). Ionomycin, KN93 and SP60125 were purchased from Sigma Chemical Co. (St. Louis, USA). Recombinant human TNFα was a gift from Dainippon Pharmaceutical Co. (Osaka, Japan). PD98059 and wortmannin were purchased from BIOMOL Research Laboratories Inc. (Plymouth Meeting, USA). SB203580 and FR167653, inhibitors of p38-MAPK, were gifts from GlaxoSmithKline and Fujisawa Pharmaceutical Co. (Osaka, Japan), respectively. H89 was purchased from Seikagaku Co. (Tokyo, Japan). Horseradish peroxidase conjugated second antibodies (anti-rabbit or anti-mouse IgG) were purchased from VECTOR Laboratories Inc.

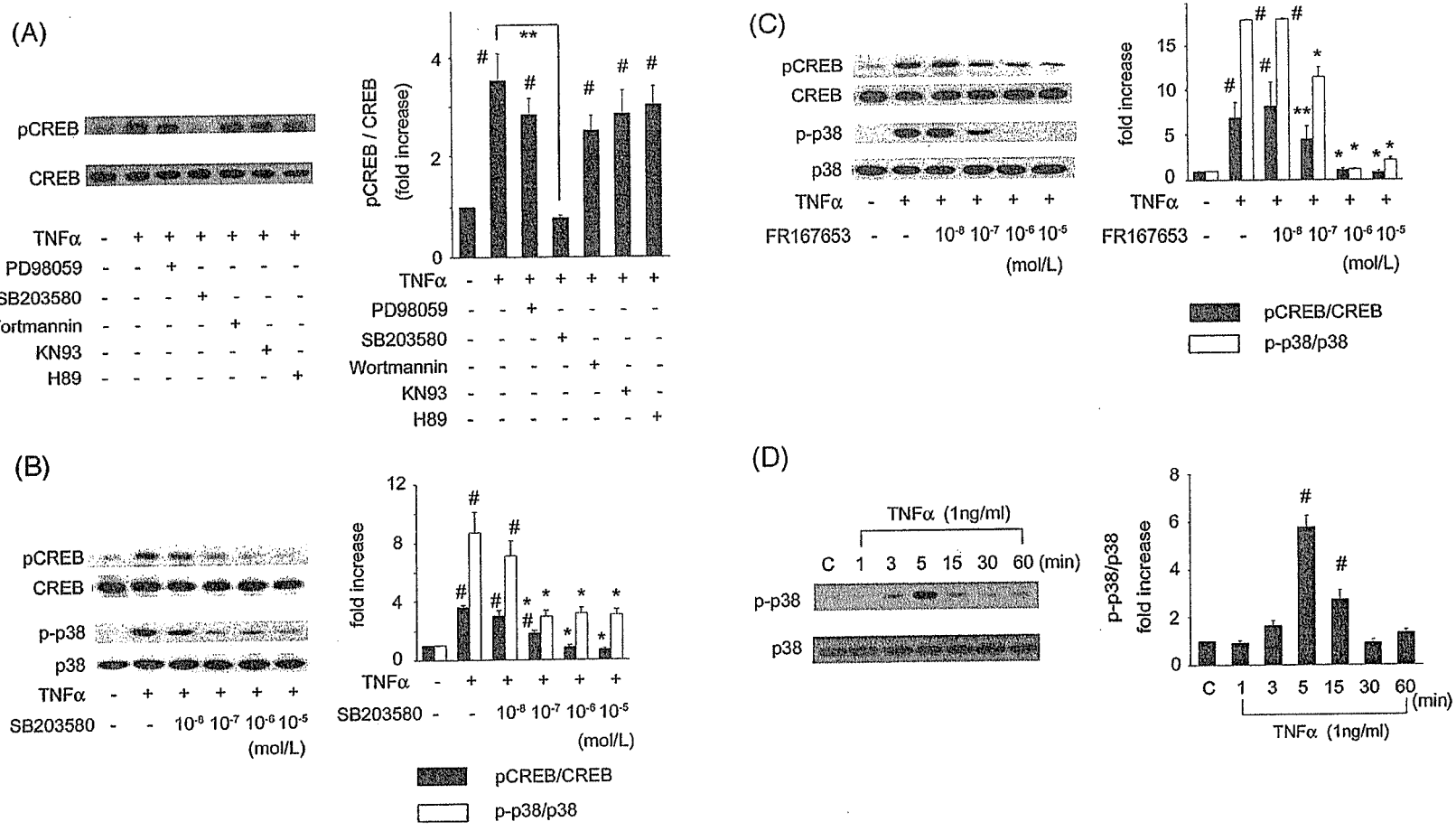

Fig. 2. *The p38-MAPK pathway mediates TNFα-induced CREB phosphorylation. A: Bovine ECs were preincubated with PD98059 (10 μmol/l), SB203580 (10 μmol/l), wortmannin (50 nmol/l), KN93 (10 μmol/l) or H89 (1 μmol/l) for 30 min and stimulated with TNFα (1 ng/ml) for 15 min. Phosphorylation of CREB was detected and analyzed as described in the legend to Fig. 1 (n = 3). The ratio of phosphorylated CREB to total CREB in TNFα-stimulated cells is shown as the relative fold increase compared with that in unstimulated cells. The values are expressed as the mean ± SEM. **p < 0.01 vs. TNFα, #p < 0.01 vs. the control. B, C: Bovine ECs were preincubated with (B) SB203580 or (C) FR167653 at concentrations varying from 10^{-8} to 10^{-5} mol/l for 30 min and stimulated with TNFα (1 ng/ml) for 15 min. D: Bovine ECs were stimulated with TNFα (1 ng/ml) for varying periods indicated in the figure. Phosphorylation of CREB and p38-MAPK was detected and analyzed as described in the legend to Fig. 1 (n = 4–6). The ratio of phosphorylated CREB or p38-MAPK to total CREB or p38-MAPK in TNFα-stimulated cells is shown as the relative fold increase compared with that in unstimulated cells. The values are expressed as the mean ± SEM. #p < 0.01 vs. the control, *p < 0.01, **p < 0.05 vs. TNFα.*

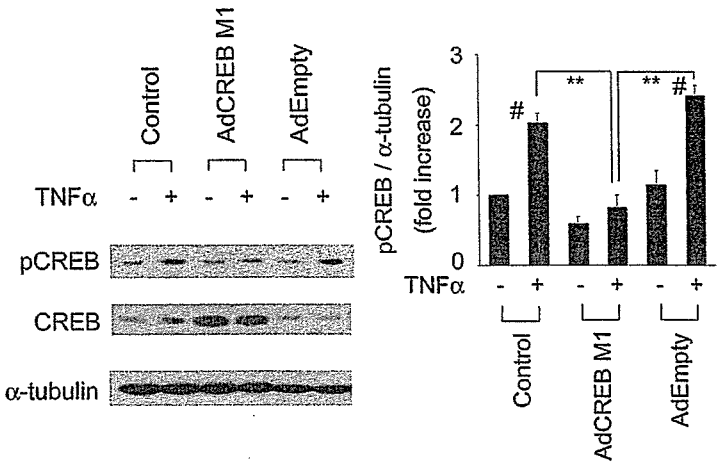

Fig. 3. *AdCREB M1 inhibits TNFα-induced CREB phosphorylation. Bovine ECs were infected with AdCREB M1 (30 MOI) or AdEmpty (30 MOI) and stimulated with or without TNFα (1 ng/ml) for 15 min. TNFα-induced CREB phosphorylation was detected by Western blot analysis (n=4). The ratio of phosphorylated CREB to α-tubulin in TNFα-stimulated cells is shown in the right panel as the relative fold increase compared with that in unstimulated cells. The values are expressed as the mean±SEM.* $^{**}p<0.01$ vs. *AdCREB M1 TNFα (+),* $^{\#}p<0.01$ vs. *control TNFα (–) or AdEmpty TNFα (–).*

(Burlingame, USA). Other antibodies used in the experiments were obtained from Cell Signaling Technology (Danvers, USA). Other chemical reagents were purchased from Wako Pure Chemicals (Osaka, Japan) unless specifically mentioned.

Cell Culture

The bovine aortic ECs were the gift of Katsuya Hirano (Kyushu University Graduate School of Medical Sciences) and grown in a humidified atmosphere of 95% air/5% CO_2 at 37°C in DMEM with 10% FBS. Passages between 5 and 12 were used for the experiments. The investigation conformed with the Guide for the Care and Laboratory Animals published by the US National Institutes of Health (NIH Publication No. 85-23, revised 1996).

Western Blot Analysis

Bovine ECs were lysed in a sample buffer (5 mmol/l EDTA, 10 mmol/l Tris-HCl, pH 7.6, 1% Triton X-100, 50 mmol/l NaCl, 30 mmol/l sodium phosphate, 50 mmol/l NaF, 1% aprotinin, 0.5% pepstatin A, 2 mmol/l phenylmethylsulfonyl fluoride and 5 mmol/l leupeptin). Western blot analyses of CREB, p38-MAPK and VCAM-1 were performed as described previously (*21*).

Adenovirus Vector Expressing a Dominant Negative Form of CREB

A recombinant adenovirus vector expressing a mutant of CREB (AdCREB M1) (*22*) in which the phosphorylation site at Ser133 was changed to alanine was a gift from Anthony J. Zeleznik (University of Pittsburgh, Pittsburgh, USA). Confluent bovine ECs were washed 2 times with PBS and incubated with AdCREB M1 or adenovirus empty vector (AdEmpty) under gentle agitation for 2 h at room temperature. Then the cells were washed 3 times, cultured in DMEM with 10% FBS for 2 days and used for the experiments. The multiplicity of infection (MOI) value indicates the number of viruses per cell added to a culture dish.

Northern Blot Analysis

Total RNA was prepared according to an acid–guanidinium–thiocyanate–phenol–chloroform extraction method. Northern blot analysis of *c-fos*, VCAM-1 and 18S rRNA was performed as described previously (*21*). The radioactivity of hybridized bands of *c-fos* and VCAM-1 mRNA, and 18S rRNA was quantified with a MacBAS Bioimage Analyzer (Fuji Film Co., Tokyo, Japan).

Preparation of Nuclear Extracts and Gel Mobility Shift Assay

The preparation of nuclear extracts and gel mobility shift assay were performed as described previously (*23*). DNA probes of AP-1 (5′-CGCTTGATGAGTCAGCCGGAA-3′) and NF-κB (5′-AGATGAGGGGACTTTCCCAGGC-3′) were end-labeled with ^{32}P γ-ATP. Ten micrograms of nuclear extracts were incubated with 1×10^5 cpm of labeled DNA probe for 30 min at room temperature and electrophoresed on 4% acrylamide gel. A fifty-fold molar excess of unlabeled DNA was added as a competitor. After electrophoresis, the